CHAPTER SIX

Modern pyroclastic fall deposits and their eruptions

, Iceland. Top
hinner, 50 km
pumice fall in

Initial statement

Pyroclastic fall deposits, their eruptions and the physical controls on their formation are now considered in detail. The classification scheme of G. P. L. Walker (1973b) characterises fall deposits by their dispersal and degree of fragmentation, and this approach is used as a framework for our description. Important volcanological assessments can also be made, because these two parameters are related to the height of an eruption column and the nature of the fragmentation process. In this chapter we also consider some surprising features of the Mt St Helens ash-fall deposits and the implications of these for plinian eruptions. We also focus on the characteristics of distal silicic ash-fall layers. Finally, the properties of welded air-fall tuffs which occur near the vent on a number of volcanoes are described. Criteria for distinguishing these from welded ignimbrites (Ch. 8) and a thermal facies model for pyroclastic fall deposits are also presented.

6.1 Introduction

The different types of pyroclastic fall deposit are ill-defined in the literature. They are described by a number of terms according to certain styles of explosive activity, named generally after individual volcanoes or volcanic areas where the activity was first observed, or of which the style of eruptions was thought to be characteristic. Examples include *strombolian*, *hawaiian*, *vesuvian* and *pelean*. One exception to this is *plinian*, which is named after Pliny the Younger, from his account to the historian

Tacitus of the eruption of Vesuvius in AD 79. This type of eruption and the resulting deposit could also have been called vesuvian. However, in the literature this refers to another style, exemplified by the basaltic eruption of Vesuvius in 1906, which involved a long-sustained gas stream with little ash being released (MacDonald 1972).

This approach to nomenclature has produced many problems. First, the style of eruption can change during the course of one eruption, and certainly during the long-term history of a volcano. For example, during its history Mt Pelée has shown a variety of styles of eruption other than pelean. It has also, for instance, experienced plinian eruptive phases (Roobol & Smith 1976). Secondly, particular eruption styles can occur in places other than the places used to name the particular eruption style. For example, hawaiian style eruptions are not just confined to Hawaii. Lastly, many deposits from historical or relatively recent eruptions have not been studied immediately after their eruption with the aim of correlating particular facies characteristics with *observed* eruption styles. In many cases, particularly with historic eruptions, the details of eruption characteristics have been *inferred* from a study of the deposits well after the eruption has ended, by people who did not observe the eruption.

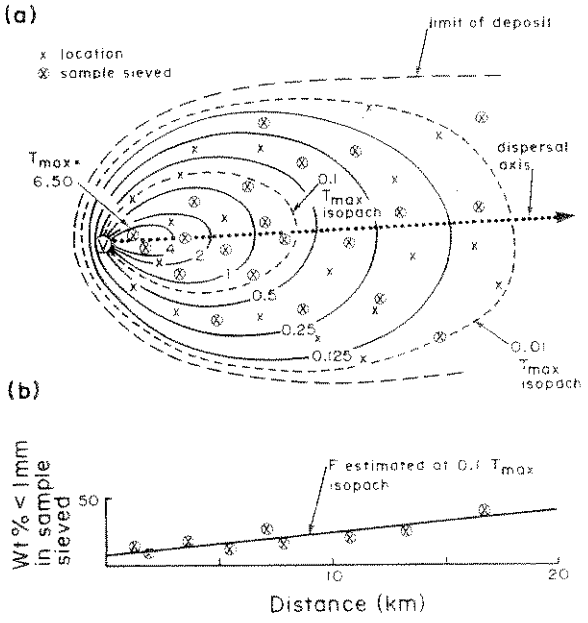

Figure 6.1 Representation of method used to obtain the two parameters *D* and *F*. See text for explanation.

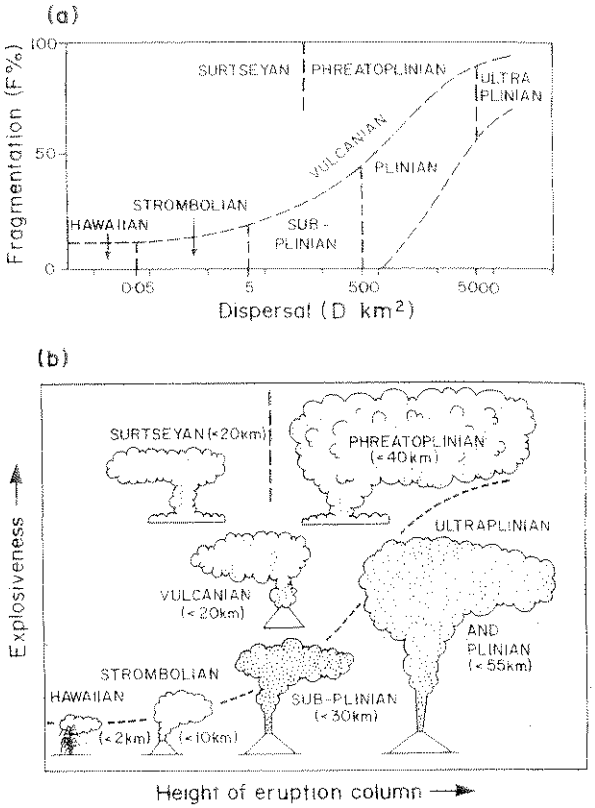

Figure 6.2 (a) *D*–*F* plot used to characterise different types of pyroclastic fall deposit (after G. P. L. Walker 1973b, and updated in J. V. Wright *et al.* 1980). (b) Cartoon explaining *D*–*F* plot in terms of eruption column height and 'explosiveness'.

However, many of the poorly defined terms are entrenched in the geological literature and it would be naive to assume that they could be abandoned. The only practical solution is to improve the definition of existing terms by more quantitative analysis applied to well preserved young deposits for which good accounts of the eruption are available. From these studies, better descriptions, that can be used as a guide to interpret equivalent deposits in the rock record, may result.

The first serious attempt to describe and classify explosive volcanic eruptions producing pyroclastic falls quantitatively was by G. P. L. Walker (1973b). Walker's approach was based on the characteristics

of the fall deposits examined in the field, and not on the characteristics of the eruptions as was generally the practice previously. This quantitative scheme (Figs 6.1 & 2) relies on accurate mapping of the distribution of fall deposits and detailed granulometric analysis to determine two parameters: dispersal (D) and fragmentation index or degree of fragmentation of the deposit (F). The empirical measure of D used is the area enclosed by the $0.01T_{max}$ isopach (where T_{max} is the maximum thickness of the deposit; Fig. 6.1a). The empirical measure of F chosen is the percentage of a deposit finer than 1 mm at the point on the axis of dispersal where it is crossed by the $0.1T_{max}$ isopach; this can only be determined from the sieve analysis of a sample collected either at this point or, more practically, obtained graphically from sieve analyses of a few samples collected near the dispersal axis (Fig. 6.1b).

G. P. L. Walker (1973b) initially characterised three types of pyroclastic fall deposit on the basis of their values of D and F: *hawaiian–strombolian*, *surtseyan* and *plinian* (Fig. 6.2a). A distinction between strombolian and hawaiian types based on D was proposed, and another distinction, based on F, between normal and violent strombolian, was also proposed. Also, *sub-plinian* was proposed as a new type, intermediate in character between strombolian and plinian. Since Walker's original plot was published, later studies have refined this, and other types of pyroclastic fall deposit have been characterised: *ultraplinian*, *vulcanian* and *phreatoplinian* (Fig. 6.2).

The D–F plot is based on the measurable characteristics of a deposit, but it also reflects some of the essential features of the eruption, even though many changes in observed style of activity may have occurred throughout eruption. For any deposit, this plot is a reflection of not only the eruption column height, since it is this which largely controls D, but also the 'explosiveness' or degree of fragmentation of the magma (Fig. 6.2b). High F-values, for instance, may result from very high intensity eruptions (high volumetric eruption rates) or magma–water interactions. This is therefore a most useful way of making volcanological assessments of, and comparisons between, pyroclastic fall deposits whose eruptions were not observed, and whose original extent is still reasonably intact.

Although the plot of D against F gives a basis for detailing types of pyroclastic fall deposits and their eruptions, it is important to point out here that further research is increasingly revealing a number of its shortcomings. The meaning of F is not as clear as was suggested above. High F-values may not prove to be the result of high degrees of fragmentation, but may also reflect 'wet' eruption plumes in which premature deposition of fines is promoted by rain-flushing. This problem is highlighted in the discussion of distal silicic ash-fall layers (Section 6.9). Also, the fields for phreatomagmatic ash-fall deposits, which are now simply divided into surtseyan and phreatoplinian, are far from satisfactory (Section 6.8).

Before we describe the different types of pyroclastic fall deposit and their eruptions, two parameters that are essential to understanding the deposition and analysis of pyroclastic fall deposits need to be discussed, these being terminal fall velocity and muzzle velocity.

6.2 Terminal fall velocity and muzzle velocity

The distance that individual pyroclastic fragments are transported from the vent is controlled by many interacting factors. The most important are the heights to which particles are taken in the eruption column, the angle of ejection, the wind strength and the terminal fall velocity of the particles.

When an object falls through the air, it accelerates until it reaches a constant or terminal velocity (TV), which is the velocity at which the force of gravity and aerodynamic drag forces are in a state of balance. Particles with smaller terminal fall velocities will travel downwind further for a given eruption column height and wind speed than larger particles with a lower terminal fall velocity. Data on the terminal fall velocities of pyroclasts are given by G. P. L. Walker *et al.* (1971) and in Appendix I.

G. P. L. Walker (1971) showed that for polycomponent pyroclastic fall deposits it is useful to

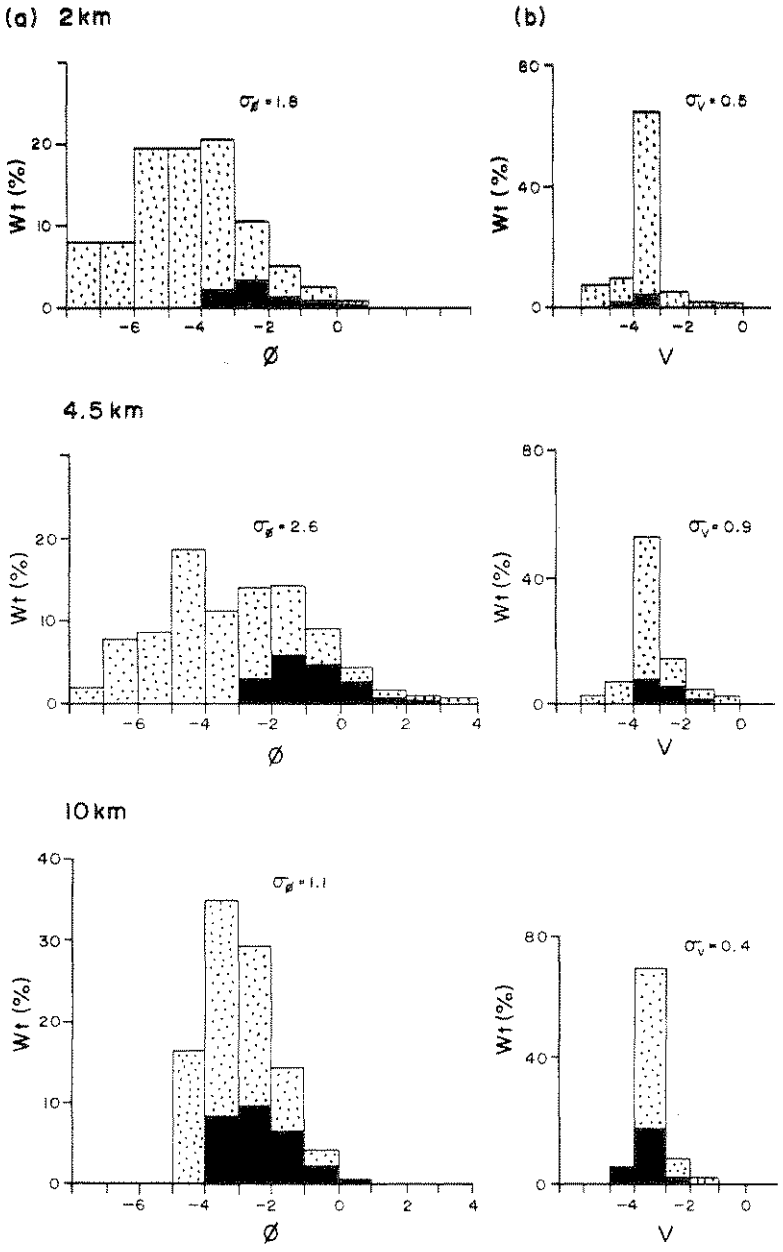

Figure 6.3 Grainsize characteristics of three samples of the Middle Pumice, a pyroclastic fall deposit on Santorini (Fig. 13.30) taken at increasing distances from the probable vent. (a) Histograms of the grainsize distributions. Grainsize distributions of air-fall deposits on a weight percentage basis are a function of the terminal fall velocity of ejecta, which is controlled by both grainsize and density. Less than 3 km from source, samples of the fall deposit contain >90 wt% pumice, and have unimodal histograms and a low σ_ϕ value. The proportion of dense components (lithics and crystals) increases from source. Between 3 and 5 km from source this results in a bimodal grainsize distribution, with a coarse mode due to pumice and a fine secondary mode due to the denser components, and an increase in σ_ϕ. At greater distances (>5 km) a decrease in the proportion of very coarse pumice clasts results in a restricted pumice size range with a mode closely corresponding to that of the dense components. The grainsize distribution is unimodal and sorting improves markedly. (b) Histograms of grainsize in weight percentages plotted against the terminal fall velocity of ejecta; V is defined as $-\log_2 TV$ where TV is the terminal velocity in metres per second. These group together all particles which fall at the same rate in the same class. By doing this, all the grainsize histograms become strongly unimodal.

plot histograms of weight percentages against terminal fall velocity, so grouping together all particles which fall at the same rate. When this is done, grainsize histograms of pyroclastic fall samples become strongly unimodal (Fig. 6.3). Median terminal fall velocity in an air-fall deposit gradually decreases with distance (Figs 6.3 & 4). The slope on the median terminal fall velocity–distance curve (Fig. 6.4) is controlled by eruption column height and wind speed. For the deposits shown in Figure 6.4, the wind speed was approximately the same, and the slope of the line is therefore a function of eruption column height.

One of the most useful physical parameters in the

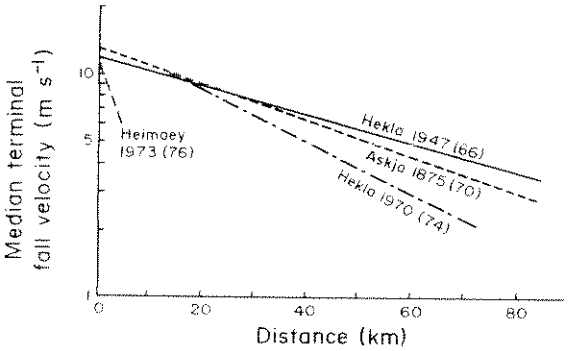

Figure 6.4 Median terminal fall velocity plotted against distance from source for some pyroclastic fall deposits. For each deposit an indication of the windspeed (in km h^{-1}) is given in parentheses. (After Self *et al.* 1974.)

comparison of explosive pyroclastic fall eruptions is the initial gas or muzzle velocity at the vent. During observed eruptions this can be determined by measuring the fall times of ballistic blocks and bombs which are unaffected by the wind, or by analysing films of eruptions. In older deposits one can measure the average maximum size of the largest fragments, and if the vent location is known these sizes can be used to estimate the minimum muzzle velocity based on the calculations of L. Wilson (1972). In L. Wilson's (1972) paper the ranges of particles ejected from vent, and the fall times of particles released from an eruption column (or ash cloud), are computed for various values of particle radius, density, launch velocity, launch angle and release height (see App. I).

For any deposit, on a plot of average maximum clast size against distance from vent, a line drawn along the top of the resulting scatter will show the maximum range of fragments of a given size (e.g. Figs 6.15 & 21, below). When maximum lithic or denser juvenile sizes are plotted. This line usually shows a sharp inflection a few kilometres from the vent, and this is thought to reflect the distance range of ballistic fragments (e.g. Figs 6.15 & 21, below). Maximum pumice sizes usually do not show this inflection, because larger pumice bombs tend to break on impact with the ground surface, and owing to their low density even the largest clasts are affected by the wind to some extent. Measurements of the largest lithic fragments are therefore going to give the most reliable estimates of muzzle velocities. For most practical purposes this is going to involve only lithics much greater than 20 cm in diameter.

6.3 Hawaiian–strombolian

These types of pyroclastic fall deposit are the products of mildly explosive eruptions of basaltic or near-basaltic magmas. Such eruptions eject scoria and relatively fluid lava spatter, and are often accompanied by the simultaneous effusion of lava (Ch. 4; Plate 3). Vents for these eruptions can be fissures or simple conduits. However, observations and theoretical considerations suggest that activity along fissures is quickly localised to a number of points (L. Wilson & Head 1981). This happened, for example, during the Heimaey eruption in 1973 (Thorarinsson *et al.* 1973). Explosive activity builds scoria (cinder or spatter cones, or both, at the vent, with scoria-fall deposits of limited areal extent and volume being deposited around and downwind of the vent. Scoria cones may be the sites of persistent activity over decades or longer, such as Stromboli (Chouet *et al.* 1974) and Northeast Crater, Mount Etna (McGetchin *et al.* 1974), but more generally they are monogenetic cones (Ch. 13) produced by what can be considered to be single eruptions lasting usually a few weeks to a few months, such as Heimaey in 1973 (Thorarinsson *et al.* 1973, Self *et al.* 1974).

6.3.1 CHARACTERISTICS OF THE DEPOSITS

Deposits of scoria cones often consist of rather poorly bedded, very coarse-grained and sometimes red (oxidised) scoria with metre-sized ballistic bombs and blocks (Figs 6.5–7). Many of the observed beds are not simply air-fall layers, but include mass-flow deposits formed by avalanching and rolling of scoria down unstable slopes as the cone built up. Such beds are laterally discontinuous. Grain flow (Ch. 10) of the loose granular material during downslope movement produces reverse grading (see Fig. 6.10c). A variety of bombs and blocks may be found: large scoriaceous fragments,

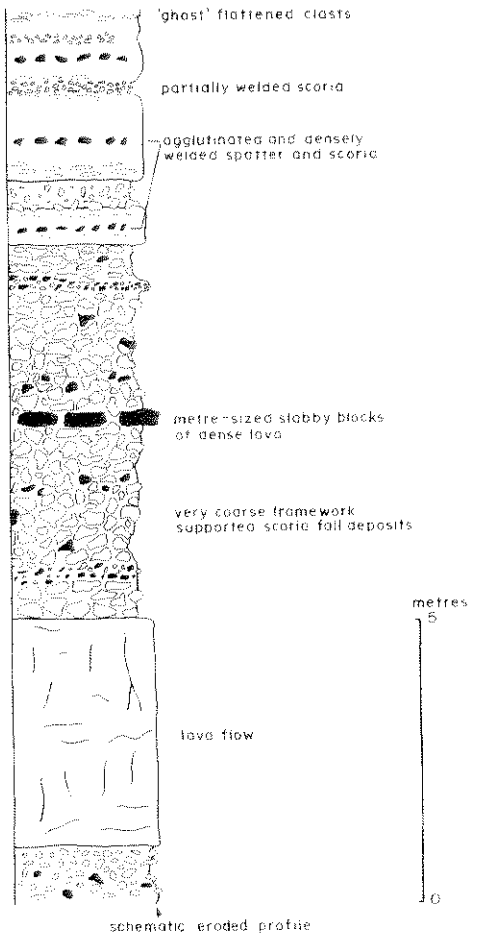

Figure 6.5 Section through uppermost part of scoria deposits at Ohakune craters, near Ruapehu volcano, New Zealand. (After Houghton & Hackett 1984.)

less well vesiculated lava having spindle and cowpat shapes, sometimes bombs with breadcrusted surfaces, and dense lava blocks and slabs. Large accessory lithics of country rock are usually uncommon, but petrologically important mantle-derived nodules may occur as 'cored' lithics with a rind of lava around them. Bomb sags are not a common feature. This is because ballistic bombs land in a thick accumulating bed of coarse, loosely packed, unstratified scoria (cf. surtseyan and base-surge deposits, where bomb sags are common because of the finer grainsizes and the often wet, plastic state of the ash pile). Layers of agglutinated lava spatter and scoria can be conspicuous (Fig. 6.8). Complete welding-together of the clasts may occur, and this is one way in which lavas may be generated (Ch. 4). Rapid accumulation of spatter and scoria is needed to produce such agglutinated and welded layers, and clastogenic lavas (see Section 6.10 on welded air-fall tuffs).

Hawaiian activity produces a much higher proportion of lava spatter at the vent, due to lava fountaining. Consequently, the formation of spatter deposits, spatter cones and ramparts at the vent (Figs 6.8g) and lava flows is likely.

The downwind fall deposits are finer-grained and composed almost entirely of scoria (Figs 6.9 & 10), and are volumetrically small (Table 6.1). Closer to the vent, ballistic bombs will be found and planar stratification defining fall units may be prominent (Figs 6.10 & 5.4a). Deposits usually contain achneliths, which are juvenile fragments with smooth, glassy surfaces formed from solidified lava spray (G. P. L. Walker & Croasdale 1972; Section 3.5). These would include the pear-shaped forms called Pele's tears, although a wide variety of shapes are possible (see Figure 3.17); the most extreme form would be the filaments of basaltic glass known as Pele's hair (Duffield *et al.* 1977). Achneliths are especially common in hawaiian scoria-fall deposits. Eruption column heights and muzzle exit velocities during hawaiian and strombolian activity are low. Consequently, scoria-fall deposits usually have a limited dispersal (*D* is low) and the fragmentation of magma is low (*F* is low in Fig. 6.11).

Table 6.1 Volume estimates of the three strombolian scoria fall deposits in Figure 6.9 (excluding volumes of the cones).

Deposit	Volume (km^3)	DRE* (km^3)
Gallarte	0.02	0.01
Serra Gorda	0.06	0.03
Cone 301	0.02	0.01

* Dense rock equivalent used for these basaltic deposits is 3.0 g cm^{-3}.

6.3.2 MECHANISMS AND DYNAMICS

In hawaiian activity the eruption column is essentially a lava *'fire'* fountain formed when jets of disrupting magma are released, almost continuously

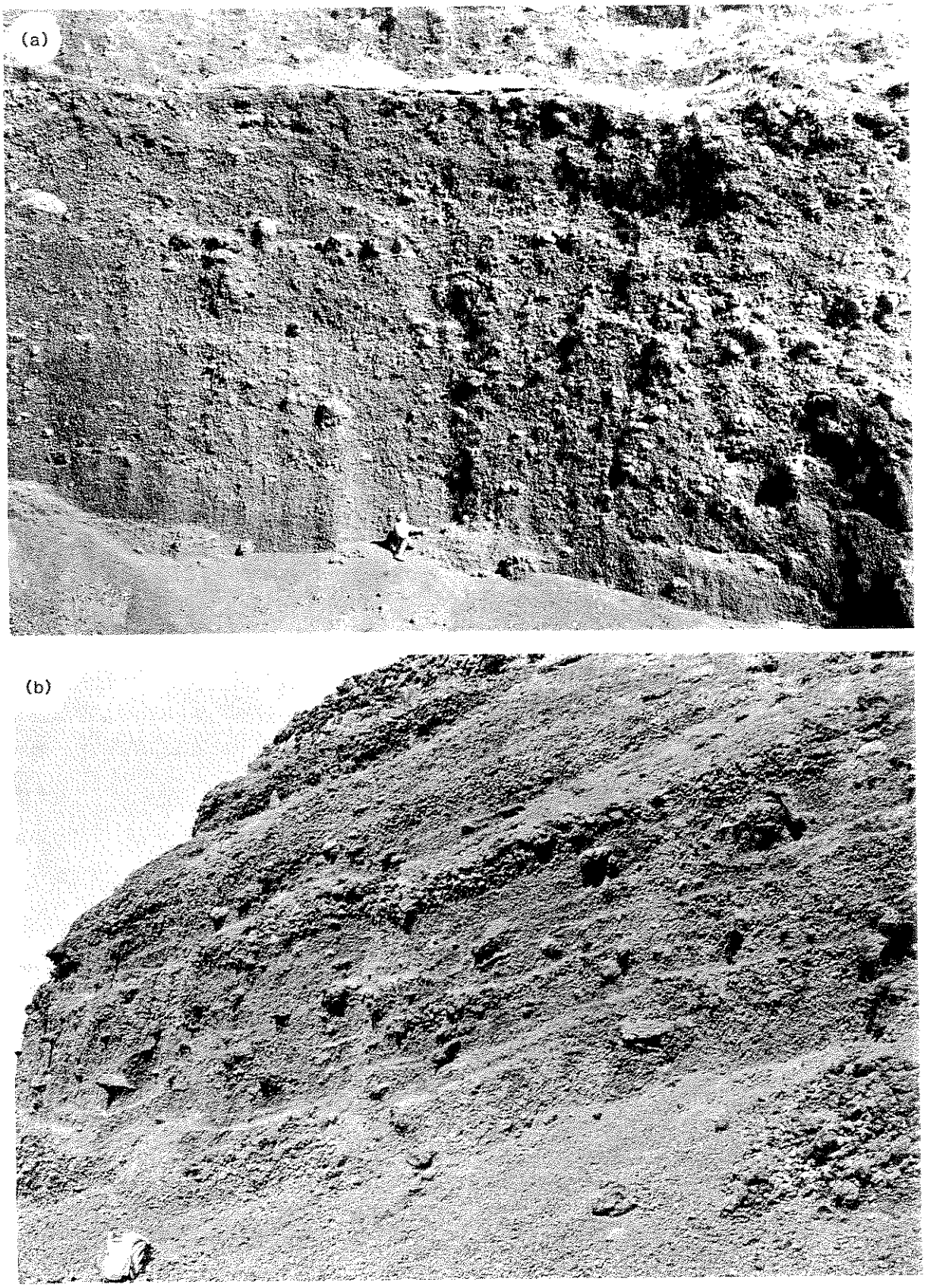

Figure 6.6 Cone-building strombolian scoria-fall deposits. (a) Mt Leura, Victoria, Australia and (b) Megalo Vourno, Santorini.

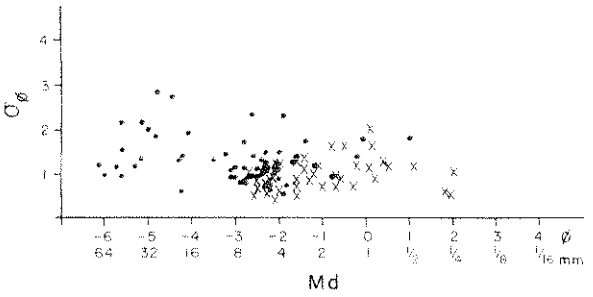

Figure 6.7 Md_ϕ/σ_ϕ plot for some strombolian pyroclastic fall deposits. Solid circles are samples collected from scoria cones, and crosses are from downwind fall deposits. (After G. P. L. Walker & Croasdale 1972, with additions for cone deposits after Houghton & Hackett (1984), and J. V. Wright *unpub. data* from Santorini.)

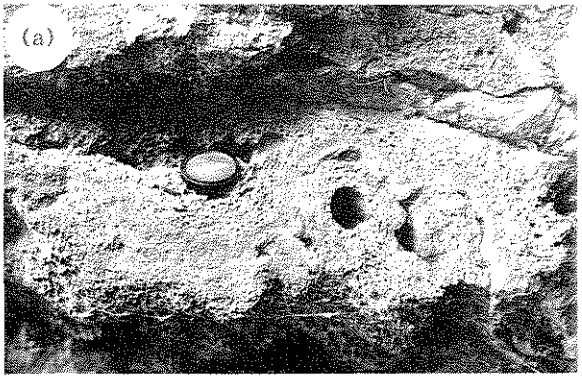

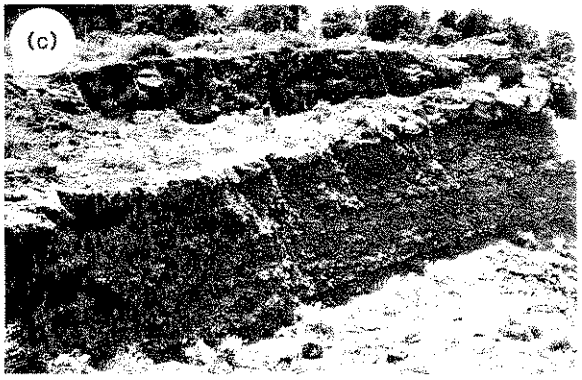

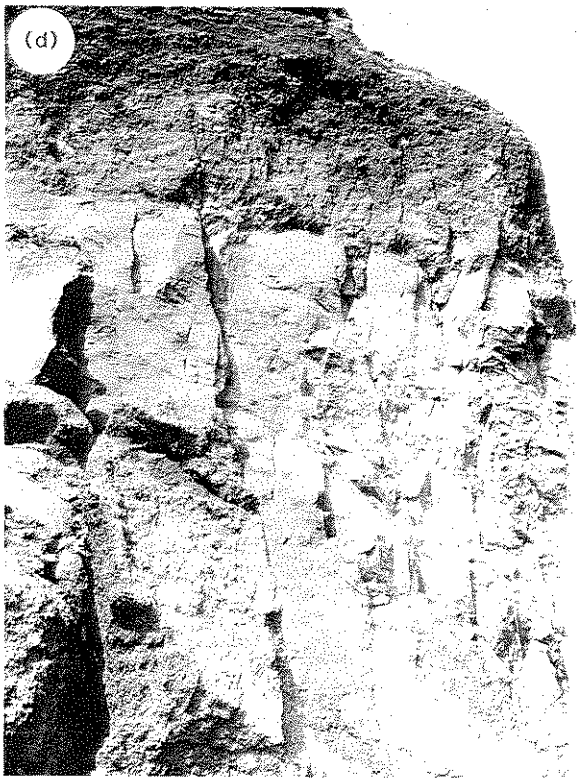

in some cases, through the vent. Lava fountain heights are generally less than about 200 m (MacDonald 1972), and in such cases magma would be ejected at velocities of a few tens of metres per second (L. Wilson & Head 1981). The predominant products of these lava fountains are large spatter pieces which fall back around the vent area. Poorly developed convective plumes above lava fountains may take the smallest ash-sized particles derived from lava spray up to heights of a few hundred metres, but all coarser fragments will already have fallen out of the column.

The mechanisms and dynamics of strombolian activity have been discussed by E. Blackburn *et al.* (1976), L. Wilson (1980a) and L. Wilson and Head (1981). Eruptions consist of a series of discrete time transient explosions separated by periods of less than 0.1 s to several hours. Explosions are thought to be generated when one or a number of large gas bubbles (<1 to >10 m in diameter) burst the magma surface (of a lava lake) at vent (E. Blackburn *et al.* 1976; Fig. 6.12a). These types of explosions can only occur in low-viscosity magmas in which bubbles can rise relatively rapidly and expand. Explosions are driven by the excessive pressure within each bubble. When each one bursts at the surface, it blasts off as pyroclasts the fragmented remains of the magma which formed the upper skin of the bursting bubble (E. Blackburn *et al.* 1976, L. Wilson 1980a). If there is a pause in activity or, as in the waning stages of an eruption, there is a pause in the activity and a crust has time to form on the magma surface, then this may be ejected during renewed bubble burst events (Fig. 6.12b). This mechanism may account for the slabby lava blocks found in some deposits (Figs 6.5 & 10b).

The pressure in the bursting bubbles is related to their size and the history of their rise through the magma, both of which, in turn, are governed by the physical properties of the magma (Ch. 2). Theoretical analysis (L. Wilson 1980a) and observed activity (Chouet *et al.* 1974, Self *et al.* 1974, E. Blackburn *et al.* 1976) suggest maximum initial gas velocities in these strombolian explosions of 300 m s^{-1}. In their analysis of 15 explosions from film of the Heimaey eruption in 1973, E. Blackburn *et al.* (1976) found the maximum initial velocity in one burst was 230 m s^{-1}, but the mean was 157 m s^{-1}. Generally, much lower initial velocities (<100 m s^{-1}) were observed in the activity of Stromboli in 1971 and 1975 (Chouet *et al.* 1974, E. Blackburn *et al.* 1976). Initial high gas thrust velocities rapidly decrease with height (up to heights of a few tens to one or two hundred metres), above which particles are transported in the upper part of the eruption column driven by convection

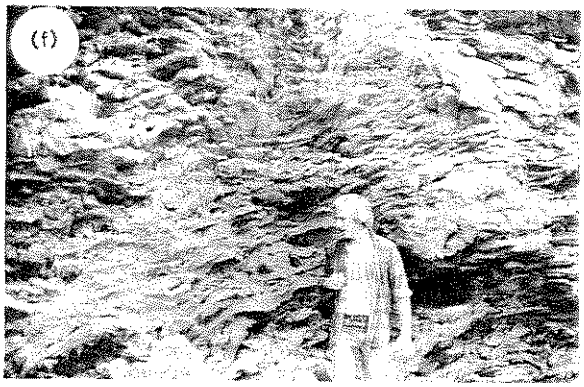

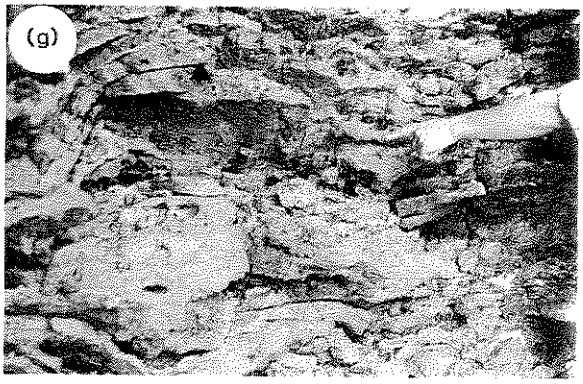

Figure 6.8 (opposite and above) Agglutinated and welded deposits from scoria cones and a spatter rampart. (a) Red Rock Complex, Victoria, Australia. Non-vesicular, banded zonation represents oxidised margins of welded spatter fragments. Interiors have vesiculated (photograph by R. Allen). (b) Coherent incipiently agglutinated scoria clasts, Mt Leura, Victoria, Australia. (c) The largely quarried strombolian cone at Ohakune, New Zealand, craters with the two agglutinated and densely welded layers shown in Figure 6.5 occurring directly below each of the benches. (d) and (e) Densely welded scoria in the cone at Balos, Santorini. Note the columnar jointing and welding zonation in (d). (f) and (g) Agglutinated lava spatter from part of a spatter rampart at the Sproul in the San Francisco volcanic field, Arizona.

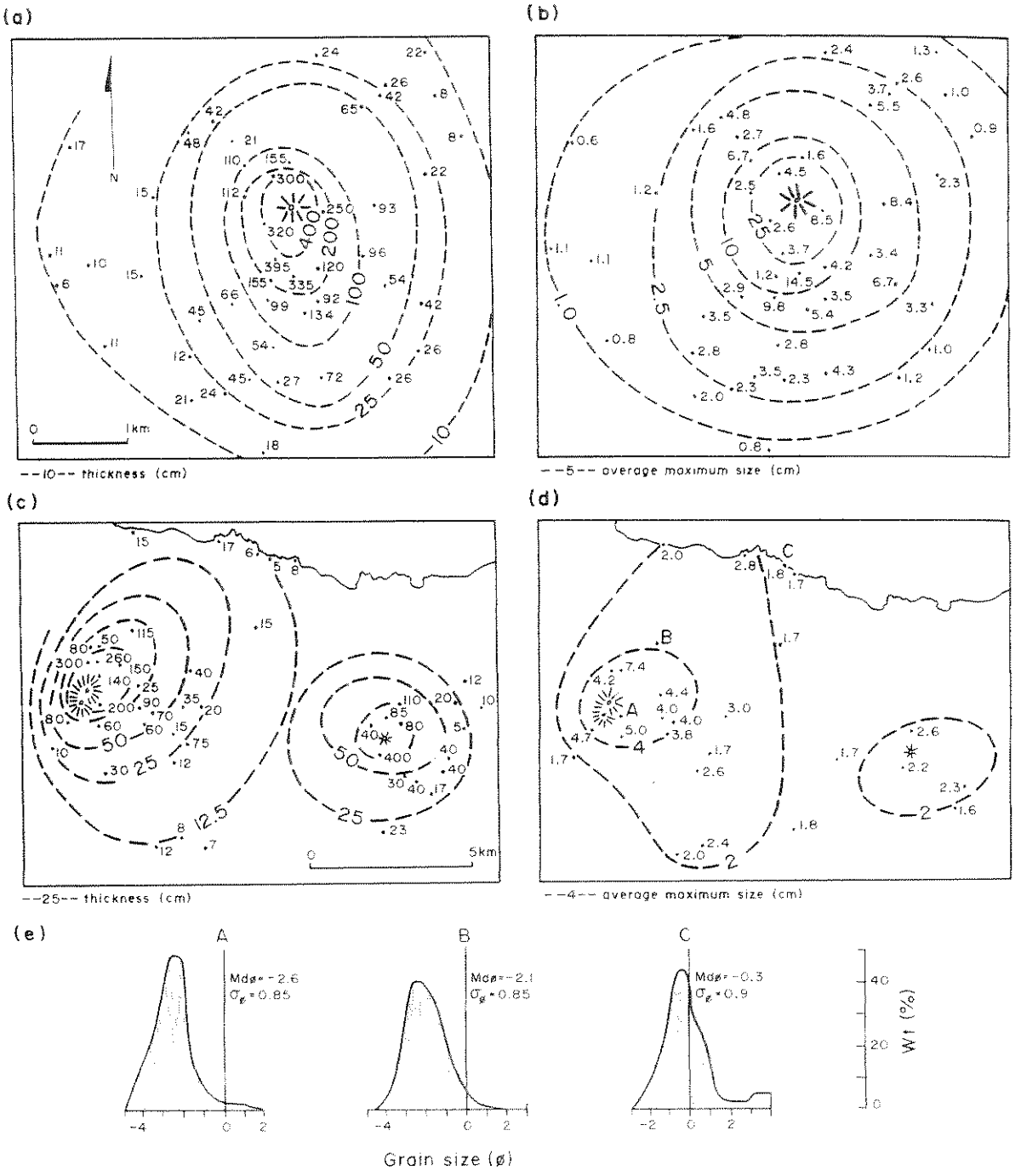

Figure 6.9 Thickness and grainsize characteristics of some strombolian pyroclastic fall deposits in the Azores. Isopleth maps show the average diameter of the three largest scoria clasts. (a) and (b) Scoria-fall deposit from the Gallarte cone, Terceira (after Self 1976). (c) and (d) Scoria-fall deposits from Serra Gorda (west) and Cone 301 (east) on São Miguel. (e) Grainsize distribution curves for the Serra Gorda deposit at the three locations in (d) (after Booth *et al.* 1978). Volumes for the three scoria-fall deposits are given in Table 6.1.

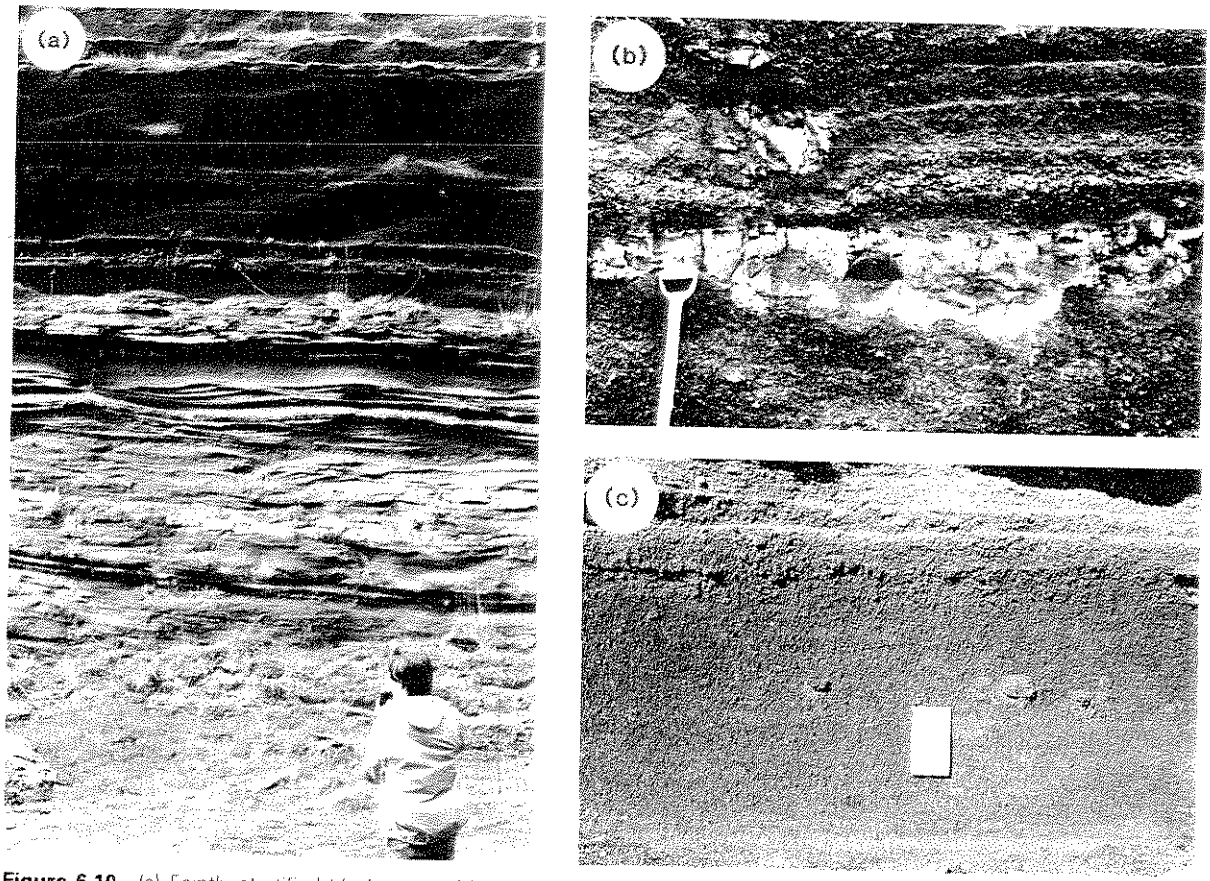

Figure 6.10 (a) Faintly stratified black scoria, Mt Leura, Camperdown, Victoria, Australia. Scoria overlies phreatomagmatic base-surge and fall deposits. (b) Cognate basaltic bomb in scoria, Mt Leura. (c) Slight reverse grading and faint stratification in scoria fall, Tower Hill, Victoria, Australia.

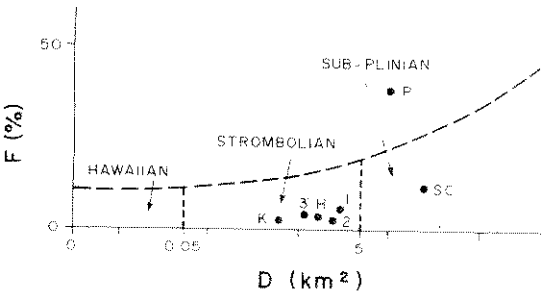

Figure 6.11 *D–F* plot for some scoria-fall deposits described in the text. 1, 2 and 3 are the downwind deposits for the Gallarte, Serra Gorda and 301 cones. H is Heimaey (1973), K is Kilauea (1959), P is Paricutin, SC is Sunset Crater (see Section 6.5 and Plate 5). (After G. P. L. Walker 1973b, Self 1976, Booth *et al.* 1978, Amos & Self *unpub. data* and sieve data of J. V. Wright on the Kilauea 1959 scoria.)

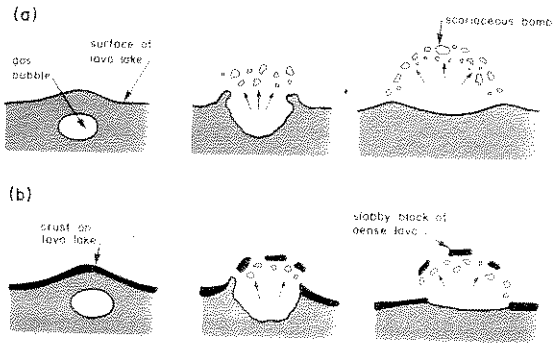

Figure 6.12 Three stages depicting the rise, expansion and bursting of gas bubbles for two contrasting situations during strombolian eruptions. (After L. Wilson 1980a.)

(E. Blackburn *et al.* 1976). If explosions occur in rapid succession (e.g. every 1–2 s), then a maintained eruption column, driven by convection, could reach heights of 5–10 km, as observed in the 1973 Heimaey eruption (see E. Blackburn *et al.* 1976). When explosions occur at longer intervals (e.g. several minutes), the convection cloud remaining after each gas thrust phase may have dissipated before the next explosion, as observed at Stromboli in 1975 (E. Blackburn *et al.* 1976). In this type of activity a fine-grained, well stratified scoria fall deposit of more limited dispersal could be built up.

6.3.3 CLASSIFICATION

The distinction between hawaiian and strombolian pyroclastic fall deposits was only tentatively defined by G. P. L. Walker (1973b) because there were limited data available at that time. There are still very few quantitative data on these deposits, especially those of hawaiian eruptions. Following G. P. L. Walker (1973b), hawaiian basaltic activity is so weakly explosive that any pyroclastic deposit which results, has a D of less than 0.05 km^2, while strombolian activity produces a deposit with a D of more than 0.05 km^2 (Fig. 6.2). This criterion, together with the distinction between the eruption mechanisms we have discussed, should only be considered as a general guide in distinguishing between hawaiian and strombolian fall deposits. Lava fountaining can reach such heights that, although observed activity would be considered typically hawaiian, the resulting deposits would be much more widely dispersed. The 1959 Kilauea Iki lava fountains reached heights of 600 m and the downwind scoria-fall deposit has a D-value of about 0.7 km^2 (Richter *et al.* 1970). By Walker's definition it is strombolian (Fig. 6.11). However, this scoria-fall deposit is composed almost entirely of achneliths or fragments of them (Fig. 3.17), and these should be a very large component of scoria-fall deposits, even of those of wide dispersal, formed by lava fountaining. During strombolian activity, if the intervals between explosions are so long that a maintained column and convective plume cannot form, then the scoria-fall deposit will be more restricted, and may be hawaiian in its dispersal characteristics. In these cases the scoria fragments will more commonly be ragged with stringy surfaces, and more typical of the strombolian mechanism of disruption of magma.

Many eruptions will also vary in observed style from hawaiian to strombolian, and vice versa. The 1973 Heimaey eruption began with lava fountains rising 50–100 m from up to 20 vents along the length of a 1.5 km fissure (Thorarinsson *et al.* 1973, Self *et al.* 1974). Later, activity became centralised and strombolian explosions took place from three vents at the northern end of the fissure, and built a scoria cone 200 m high, from which lava continually flowed. Perhaps where detailed analysis of a deposit is possible (i.e. exposure allows many vertical sections of a deposit to be studied) the dispersal characteristics of individual fall units corresponding to different phases could be determined. However, in most cases, it is only possible to determine the finite characteristics of a deposit, which in the case of Heimaey, show it is typically strombolian (Fig. 6.11).

Finally, G. P. L. Walker (1973b) described some scoria-fall deposits with unusually high values of F as 'violent strombolian'. The scoria-fall deposit erupted from Paricutin volcano, Mexico, is of this type (Fig. 6.11). Activity during this eruption continued sporadically for nine years. Ground water possibly gained access to the magma at times, but not in sufficient amounts to produce a surtseyan fall deposit (Section 6.8).

6.4 Plinian

Plinian pyroclastic fall deposits are a common product of highly explosive eruptions of high viscosity magmas. These are generally andesitic to rhyolitic, or phonolitic and trachytic compositions, but rare basaltic scoria-fall deposits which have plinian dispersal patterns are known (S. N. Williams 1983, G. P. L. Walker *et al.* 1984). The characteristics of plinian pumice fall deposits and their eruptions are now fairly well defined, and the extensive literature about these has been reviewed by G. P. L. Walker (1981b).

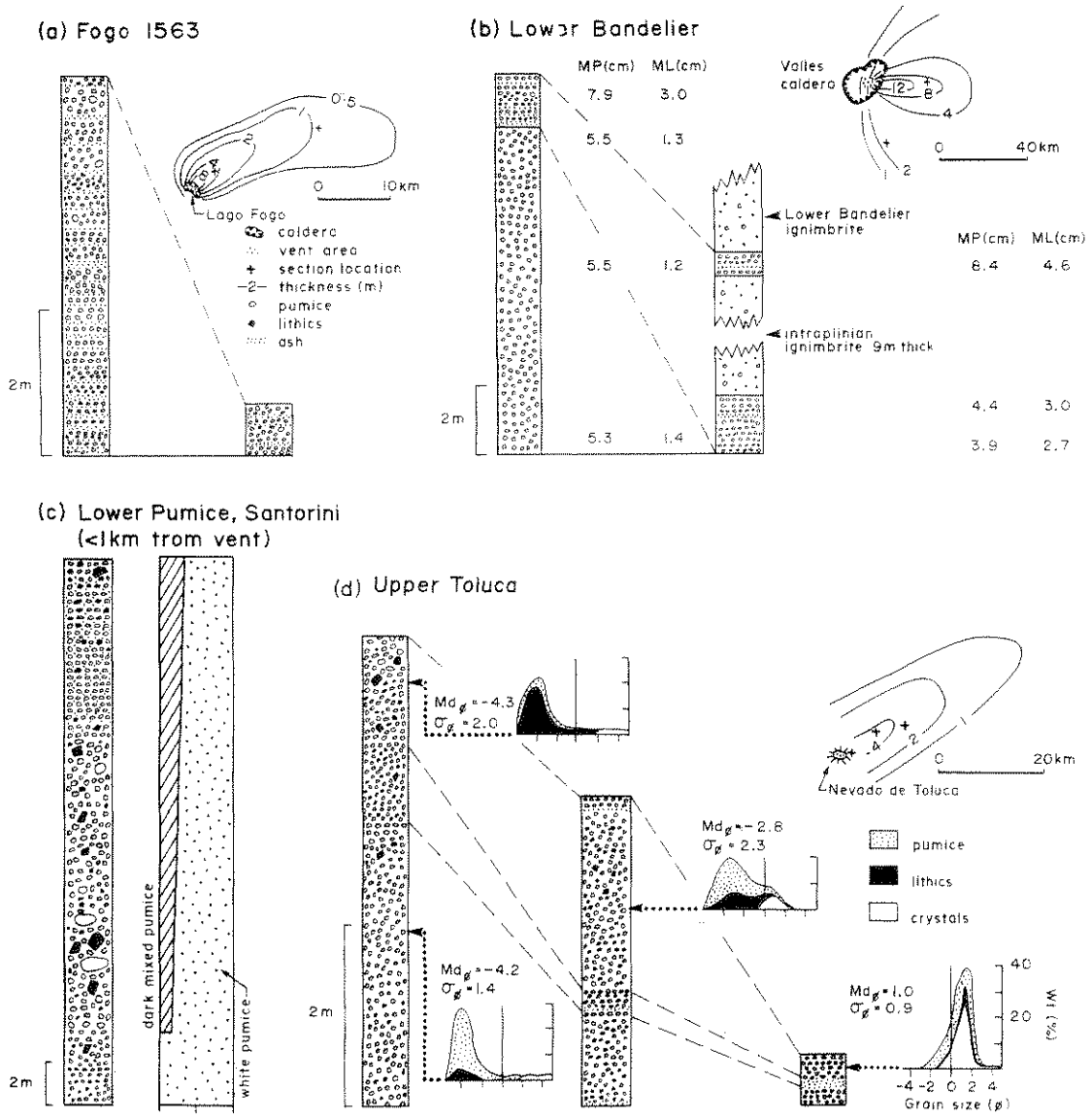

Figure 6.13 Some features of plinian pumice-fall deposits. ((a) After G. P. L. Walker & Croasdale 1971, (b) Self & Wright *unpub. data*, (c) J. V. Wright *unpub. data* and (d) Bloomfield *et al.* 1977.)

6.4.1 GENERAL CHARACTERISTICS

During plinian eruptions large volumes of pumice are ejected and extensive pumice-fall deposits are produced. These are the most impressive types of pyroclastic fall deposit found in the field (Figs 6.13 & 14). The deposits of individual eruptions may attain thicknesses near vent of 10–25 m (Fig. 6.13c); maximum thicknesses can be much smaller, but would rarely be greater. Near-vent deposits are generally homogeneous and can be very coarse, containing large pumice fragments of several tens of centimetres, and metre-sized ballistic lithic blocks. More rarely, larger pumice bombs are found, but in most cases fragmentation on impact destroys these. Away from the vent deposits become thin and fine-

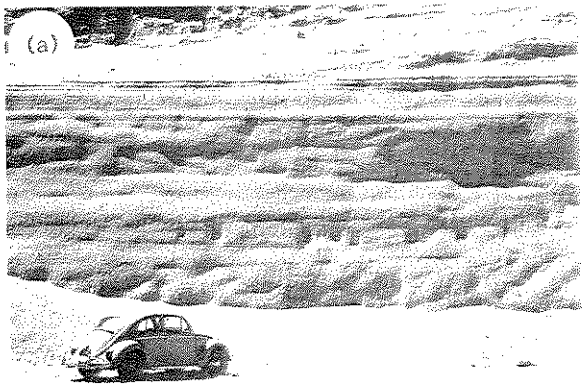
(a)

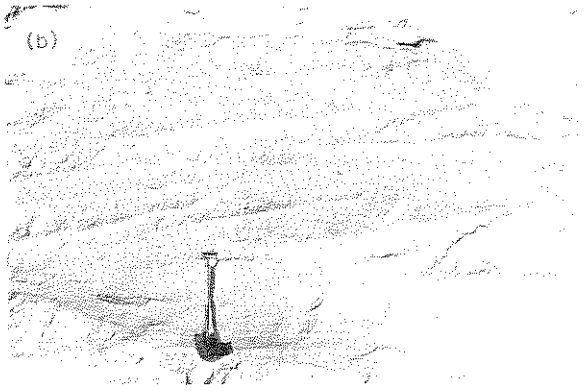
(b)

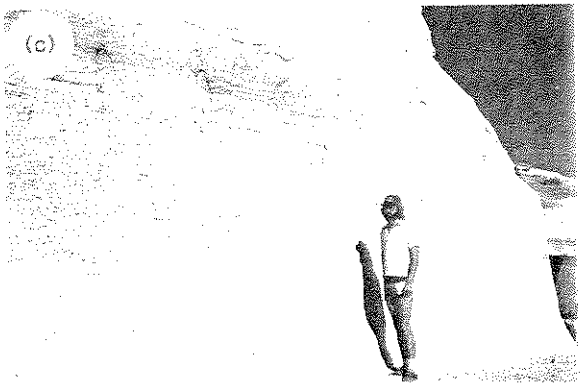
(c)


(d)

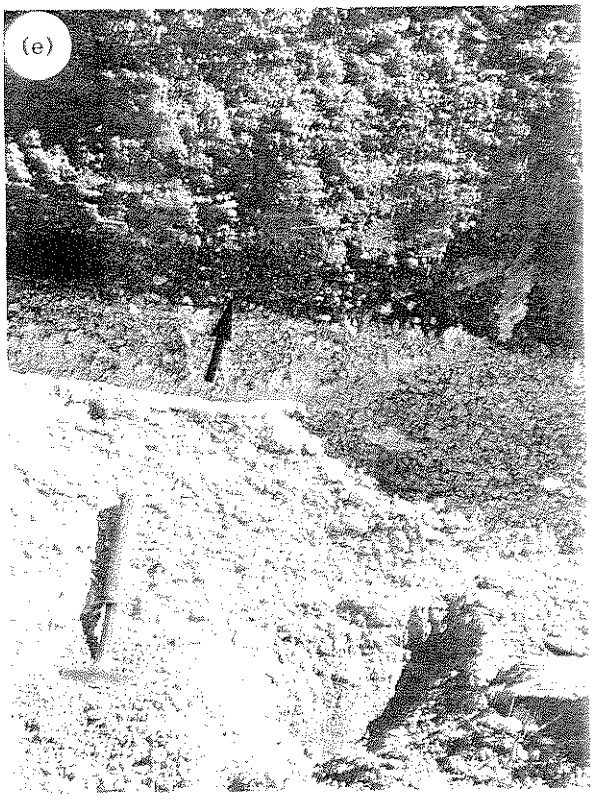
(e)

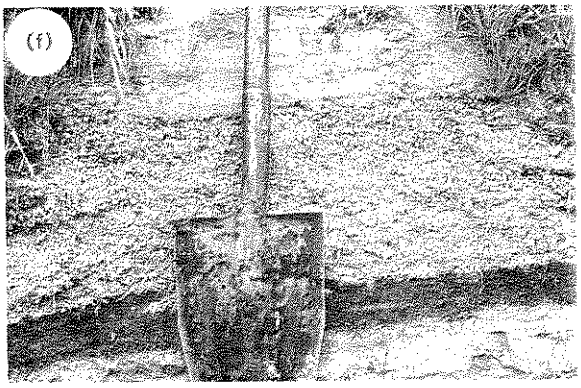
(f)

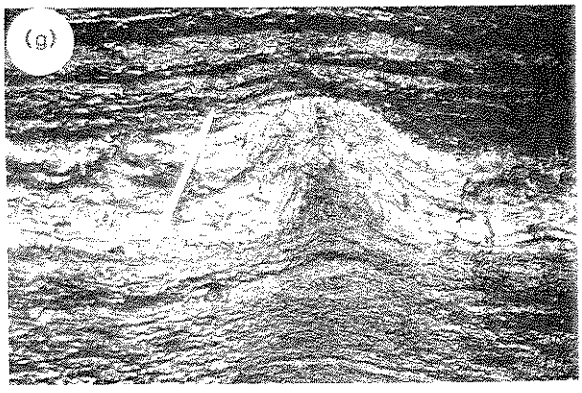
(g)

grained, and change in character, and it is the documentation and analysis of these changes that can be so important in making volcanological interpretations. Plinian pumice-fall deposits are a common eruptive product of all large rhyolite volcanoes, but are also frequently found as products of a range of andesitic and alkaline stratovolcanoes.

A few plinian eruptions are known to have occurred this century, and examples that are well documented are the eruptions of Hekla, Iceland, in 1947 (Thorarinsson 1954, 1968) and Santá Maria, Guatemala, in 1902 (Rose 1972b, S. N. Williams & Self 1983). Another example is the 1932 eruption of Quizapú in the Chilean Andes (Larsson 1936), but there has not been a more recent study of the deposits of this eruption. Quite a number of plinian eruptions have occurred in earlier historic times, and the deposits of the following examples have received detailed attention: the eruptions of Askja, Iceland in 1875 (Sparks *et al.* 1981), Tarumai, Japan in 1667 (T. Suzuki *et al.* 1973), Fogo, São Miguel, the Azores in 1563 (G. P. L. Walker & Croasdale 1971; Fig. 6.13a) and, better known because of their archaeological significance, Vesuvius in AD 79 (Lirer *et al.* 1973) and the Minoan (1470 BC) eruption of Santorini (Bond & Sparks 1976). Historical records have complemented some of these studies, and have provided evidence of the duration of these events. As well as these, much of our data on this type of activity stems from a number of studies on older plinian deposits which abound in the Quaternary record, e.g. Booth (1973), Bloomfield *et al.* (1977), Booth *et al.* (1978), G. P. L. Walker and Croasdale (1971), G. P. L. Walker (1981c), G. P. L. Walker *et al.* (1981d), and see the review of G. P. L. Walker (1981b).

All of the historical plinian eruptions mentioned above seem to have taken place from central vents, and most of the older deposits studied have been mapped to 'circular vents', which are generally assumed to be located above cylindrical conduits. There is no doubt that some of these vents are aligned along linear fissures or ring fractures, but activity from different vents in many cases can be shown to be separated by long intervals, recognised, for instance, by soils between their different fall deposits. However, detailed mapping by Nairn (1981) in the Okataina rhyolitic centre in New Zealand has shown that many plinian fall deposits and associated ignimbrites were erupted in simultaneous or sequential activity from multiple vents along fissures. These eruptions were often spread along lengths of fissure more than 10 km long but, as in basaltic fissure eruptions, activity seems to have been restricted to definite points. Vent types for large explosive silicic eruptions, during which plinian activity may lead to ignimbrite formation, are discussed in Chapter 8.

When mapped out, plinian pyroclastic fall deposits are extensive sheet-like deposits. They have a large dispersal, and D is >500 km^2 (Fig. 6.2). However, fragmentation of the magma is only moderate, and F is small to medium. Sizes of ballistic lithic blocks near the vent imply that muzzle velocities of 400–600 m s^{-1} occur (L. Wilson 1976; App. I). These suggest that very high rates of magma discharge are possible which in turn lead to the 'stoking up' of very high eruption columns, and evidence suggests that column heights >20 km should be common during this type of activity (L. Wilson 1976, L. Wilson *et al.* 1978; Ch. 5). In the events this century, the height of the column of the 1947 Hekla eruption reached 24 km, and that of Santá Maria in 1902 reached at least 28 km (S. N. Williams and Self 1983; Table 5.1). It

◀ **Figure 6.14** Plinian pumice-fall deposits. (a) The very impressive Lower Bandelier plinian deposit 30 km downwind from the vent. This is the section illustrated in Figure 6.13b; overlying the stratified top of the pumice-fall deposit is ignimbrite. (b) Upper Bandelier plinian deposit; note the finely stratified fall unit at the base. (c) Plinian fall deposit at the base of the Bishop Tuff, California. Darker layer is a surge deposit which is overlain by ignimbrite. (d) Plinian deposit erupted 26 000 years BP from the Okataina rhyolitic centre, New Zealand. (e) Compositionally zoned pumice fall on Tenerife, white pumice is phonolitic, dark (arrowed) is latite which is overlain by a soil. Hammerhead rests on base of the deposit (photograph by J. A. Wolff). (f) Reversely zoned basaltic to rhyolitic plinian deposit erupted 17 000 years BP from Tarawera, New Zealand. (g) Distal plinian layer deformed by soft-sediment loading; this was erupted from Hekla volcano and is stratigraphically below the two deposits shown in Plate 6.

Table 6.2 Volume estimates of some plinian deposits (highlighting some of the largest known in modern volcanic successions).

Deposit	Volume (km^3)	DRE* (km^3)	Composition
Shikotsu	100	24	rhyolite
Lower Bandelier	100	24	rhyolite
Upper Bandelier	70	17	rhyolite
La Primavera B (95 000 years BP)	50	14	rhyolite
La Primavera D	2	0.6	rhyolite
La Primavera E	2.6	0.7	rhyolite
La Primavera J	12	3.4	rhyolite
Upper Toluca (11 600 years BP)	9	4.0	andesite
Waimihia (3400 years BP)	29	7.1	rhyolite (mixed)
Hatepe (AD 186)	6.0	1.5	rhyolite
Vesuvius AD 79 (Pompeii pumice)	6.0	1.4	phonolite (zoned)
Askja 1875	1.0	0.2	rhyolite (mixed)
Santa Maria 1902	20	8.5	dacite (mixed)
Hekla 1947	0.4	0.1	andesite
Mt St Helens 1980	1.1	0.2	dacite

* A dense rock equivalent of 2.5 g cm^{-3} is used.

Data are taken from G. P. L. Walker (1981b, c) except the Bandelier plinian deposits (Self & Wright *unpub. data*), Santa Maria (S. N. Williams & Self 1983) and Mt St Helens 1980 (Sarna-Wojcicki *et al.* 1981). All volumes except Mt St Helens 1980 are calculated from the area plots shown in Figure 6.18 and the method of G. P. L. Walker discussed in Appendix I.

is the high eruption column in this type of activity that leads to the wide dispersal of plinian deposits. Volumes of plinian-fall deposits range from about 0.1 to >50 km^3 (Table 6.2). Examples of small-volume deposits would be those from Hekla in 1947 and Mt St Helens in 1980. Much larger deposits are known further back in the record: some of the biggest are the Shikotsu pumice deposit in Japan and the Lower Bandelier plinian deposit, both about 100 km^3. Volumes can be estimated from isopach maps of the deposits by various methods, and these are discussed in Appendix I.

6.4.2 INTERNAL AND LATERAL CHANGES

Many deposits at first sight appear to be fairly homogeneous, or at least their lower parts do (Figs 6.13 & 14), and this is thought to reflect continual fall-out from a downwind plume continually fed by a continuous gas blast. They are predominantly composed of juvenile material: pumice, glass shards and, when the magma is porphyritic, free crystals. However, significant departures from homogeneity can occur in detail. Reverse-grading of larger pumice fragments seems to be common, as is internal stratification. Accessory lithics, derived from the conduit wall, can be important in certain parts of a deposit. Also, a number of plinian fall deposits are now known to be compositionally zoned, or to contain mixed pumice clasts (Figs 6.13c, 14e & f).

Reverse grading of larger pumice clasts has been described from a number of deposits (e.g. Lirer *et al.* 1973, Bond & Sparks 1976, Bloomfield *et al.* 1977). This is usually more likely to be found at distances of several to a few tens of kilometres from the vent, and outside these limits may be only slightly developed, or it may not occur. Nearer the vent (<5 km) deposits are often so coarse-grained that it is very hard to detect any grading, and more distally (>50 km) deposits may be too fine-grained. Many deposits also show an upward increase in the proportion and size of accessory lithic clasts. Reverse grading of both pumice and lithics must reflect some process occurring at the vent affecting the eruption column with time. This will be considered further in Section 6.4.3.

Internal stratification also occurs. It is usually best developed towards the vent, and is commonly and significantly found towards the top of some deposits (Figs 6.13 & 14). Further away from the vent such stratification disappears. Stratification

varies from a crude internal layering to distinct mappable fall units, although dividing deposits up into fall units can be rather subjective.

There are a number of causes for the development of stratification. Eruptions are probably not truly continuous, but pulse-like. Slight fluctuations in muzzle velocity and discharge rate will cause particles of a given size and terminal fall velocity to be released from different heights. A pulsating column such as this would produce faint layering in a fall deposit (e.g. Fig. 6.14d); this type of stratification would rapidly disappear away from the vent as pyroclasts quickly mixed downwind. More-significant changes in activity are probably needed to cause distinct fall unit breaks. Activity could temporarily cease, caused, for instance, by blockage of the conduit by collapse of the vent walls. During such breaks, fine ash may settle out from the previous column as it dissipates, forming a thin, discrete fine-grained fall unit overlying the deposit of the maintained column. When activity recurs, the next fall unit may at first be rich in lithic fragments, as lithic fragments that blocked the vent are reamed out. Smaller collapses of the vent wall may just cause an increase in the amount of lithics taken into the column, and these would be recognised as a layer of lithics, perhaps within a fall unit. Obviously, there are a number of scenarios that can be considered. All of the above mechanisms involve changes at the vent affecting the behaviour of the eruption column. However, stratification can also be generated away from the vent. Rain flushing could prematurely bring down fine ash from the plume in localised areas while the eruption continues. Such fine-grained fall units will have isopachs which do not close on the vent (their distribution and thickness is related to the distribution and intensity of the rain shower), and they may contain accretionary lapilli (G. P. L. Walker 1981d).

In the above we have only discussed the generation of stratification by the 'random' processes which could occur at any time during a plinian event. The stratification and fall units found at the top of some deposits may, however, be related to more-significant changes that are developing with time as the plinian eruption continues. Sometimes pyroclastic flow and surge deposits are found interbedded between separate fall units, particularly in proximal areas (e.g. Self *et al.* 1984). The deposits of these flows can be traced laterally into fine ash-fall deposits. In many cases plinian deposits are overlain by ignimbrite, and it seems that there is a continuum from a plinian eruption column to a pyroclastic flow-forming or collapsing column. The stratification at the top of many plinian deposits may reflect instabilities in the column before wholesale collapse occurs to generate ignimbrite.

Compositionally zoned plinian pumice-fall deposits are now known to be common, and invariably these show an upward vertical increase in the proportion of a more basic juvenile component (Figs 6.13c & 14e). Rarer examples are known where this type of zonation is reversed (Fig. 6.14f). The boundary between zones can be gradational or very abrupt. This is commonly not marked by grainsize differences, showing that the discharge of magma was steady, although the composition of the magma was changing. In some cases there is an almost complete change in magma types, in others there is just a slight change in the proportion of the two types. Streaky mixed-pumice clasts are common in some deposits, and indicate mechanical mixing of the magma types before eruption (e.g. Fig. 3.22). Some deposits, although not distinctly zoned, can have a significant proportion of mixed pumice, e.g. the Askja 1875 deposit (Sparks *et al.* 1981). Aspects of the role of magma mixing in explosive volcanism have already been discussed in Chapter 3 (and see Ch. 8). It may be that injection of more basic magma into high-silica magma chambers triggered a number of plinian eruptions (Ch. 3).

Many of the overall downwind and lateral changes in the character of plinian fall deposits are now well established. These are:

(a) decrease in thickness,
(b) decrease in maximum grainsize (pumice and lithics),
(c) decrease in median grainsize (increasing M_ϕ values),
(d) increase in sorting (decreasing σ_ϕ values),
(e) changes in component population and
(f) decrease in median terminal fall velocity.

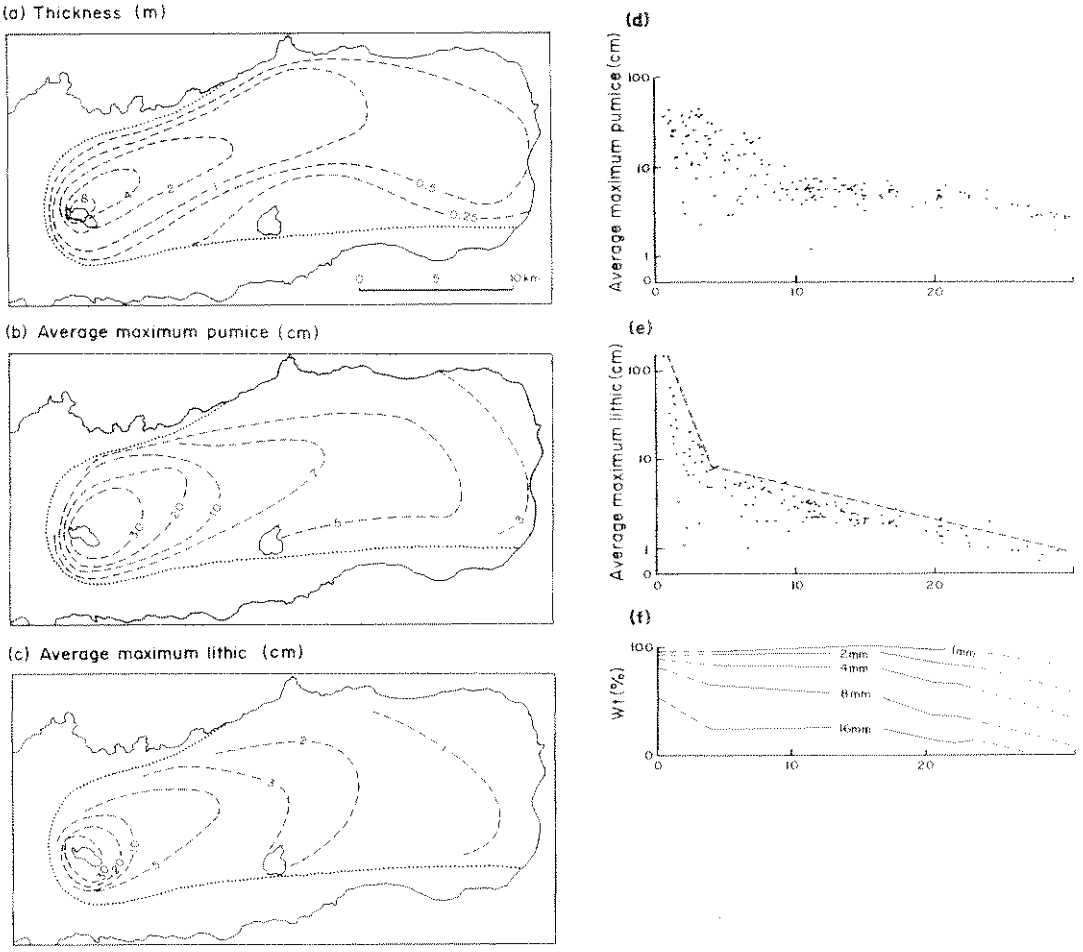

Figure 6.15 The 1563 Fogo plinian pumice-fall deposit erupted from the volcano Água de Pau (with a caldera now occupied by Lago Fogo) on São Miguel (see also Fig. 6.13a). (a) Isopach map. (b) and (c) Maximum size isopleth maps using the average diameter of the three largest clasts for pumice and lithics, respectively. (d)–(f) Maximum pumice, lithic and total grainsize variation with distance from vent. (After G. P. L. Walker & Croasdale 1971.)

There are various forms in which these data are presented, e.g. maps or graphically (Figs 6.15–6.19). However, all illustrate the dispersal characteristics of the fall deposit.

The best way of comparing thickness, maximum grainsize and median grainsize is to make 'area plots' (G. P. L. Walker 1980, 1981b, G. P. L. Walker *et al.* 1981d; Figs 6.18 & 19). These show the areas enclosed by isopachs of thickness, or isopleths of maximum or median grainsize. These plots are useful for comparing the dispersal characteristics of different plinian deposits, and can also be used to classify different types of pyroclastic fall deposits instead of using *D*–*F* plots. In practice, it is easier to determine the areas enclosed by maximum grainsize isopleths (Fig. 6.19) than determining *D*–*F* values. The value of *D* is sensitive to the choice of T_{max} (Fig. 6.1b), which may have to be extrapolated from data collected at locations some distance from the vent. G. P. L. Walker (1981b) indicated that when categorising a deposit as plinian or not, more reliability should be

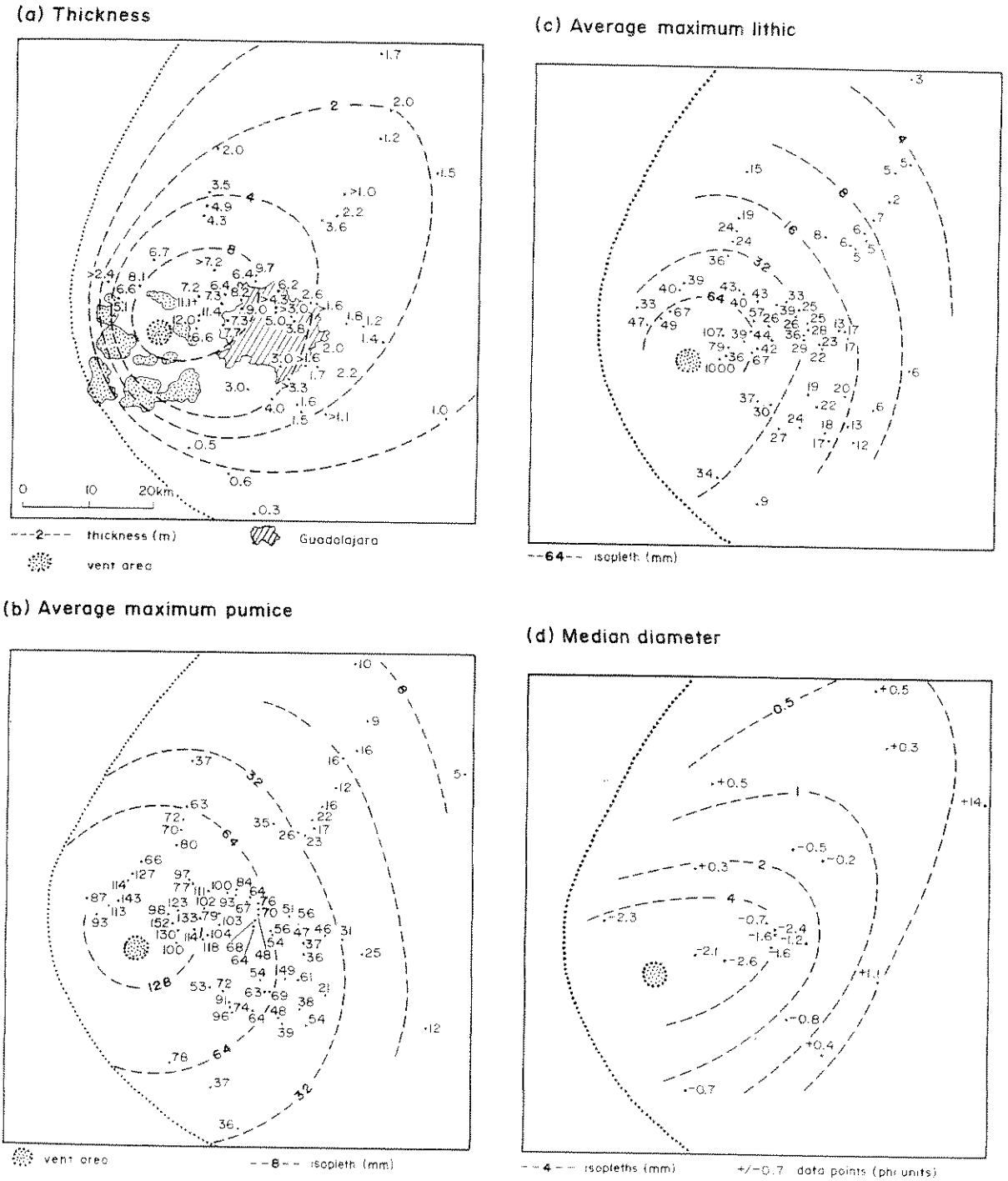

Figure 6.16 Thickness and grainsize characteristics of La Primavera B plinian pumice-fall deposit erupted from La Primavera rhyolite volcano, Mexico. (After G. P. L. Walker *et al.* 1981d.)

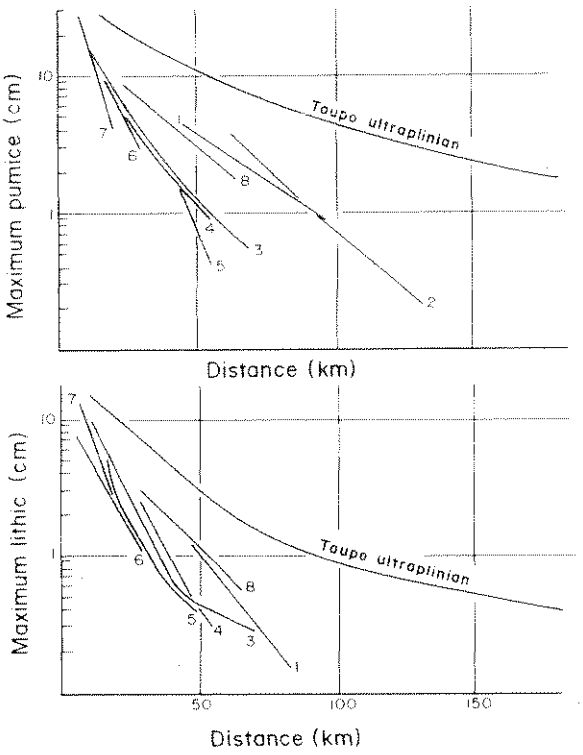

Figure 6.17 Variation in maximum pumice and lithic diameter (average of the largest three or five clasts) with distance from vent for some plinian pumice-fall deposits and the Taupo ultraplinian deposit. 1 Shikotsu; 2 Askja (1875); 3 Pompeii; 4 La Primavera B; 5 Upper Toluca; 6 Fogo (1563); 7 Fogo A; 8 Lower Bandelier. (After G. P. L. Walker 1980 and Self & Wright *unpub. data* on the Lower Bandelier plinian deposit.)

placed on the plinian field in area plots of isopleths maximum pumice (MP), maximum lithics (ML), and median (Md) grainsizes than on *D*–*F* plots.

6.4.3 MECHANISMS AND DYNAMICS

From observations of historic eruptions and analysis of plinian-fall deposits, coupled with theoretical analysis and modelling, a large amount is known about the mechanisms and dynamics of this type of eruption. The development of ideas on plinian eruption mechanisms can be traced in a number of papers based largely on the work of Lionel Wilson (L. Wilson 1976, 1980a, L. Wilson *et al.* 1978, 1980, Sparks 1978a, and Sparks and L. Wilson 1976). Plinian eruptions are essentially relatively steady, high-energy events in which a continuous, turbulent flow of fragmented magma and gas is released through a conduit to the atmosphere.

We have already discussed how fragmentation of magma occurs during this type of eruption in Chapter 3 (Fig. 3.4). Gas bubbles in rising salic magma nucleate and grow until the volume occupied by bubbles has increased (by pressure decrease and gas exsolution) to a critical value of about 70–80%, when magma disrupts (Sparks 1978a). Rapid acceleration of the disrupted magma then occurs through the conduit, which is essentially a fracture propagated to the Earth's surface from the magma chamber. The maximum velocity of the mixture as it leaves the vent is a function of gas pressure at the

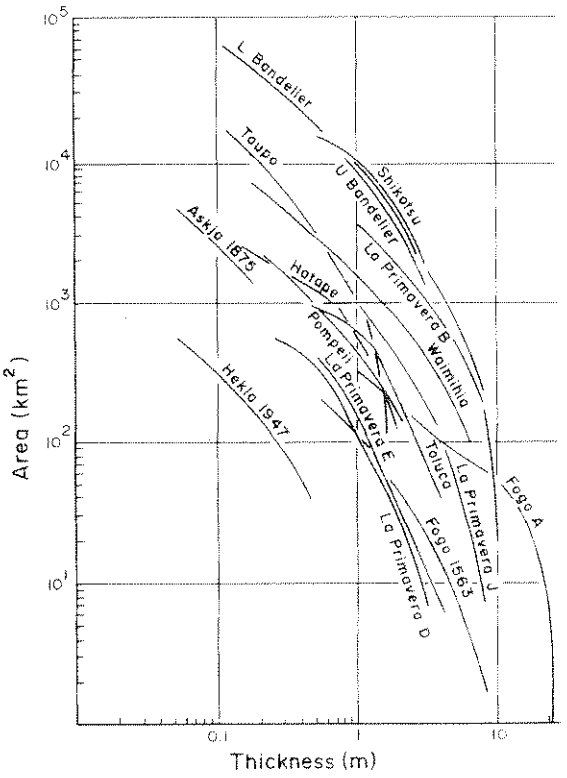

Figure 6.18 Plot of the area enclosed by each isopach against thickness for some plinian fall deposits and the Taupo ultraplinian deposit. (After G. P. L. Walker 1980, 1981b and Self & Wright *unpub. data* on the Bandelier plinian deposits.)

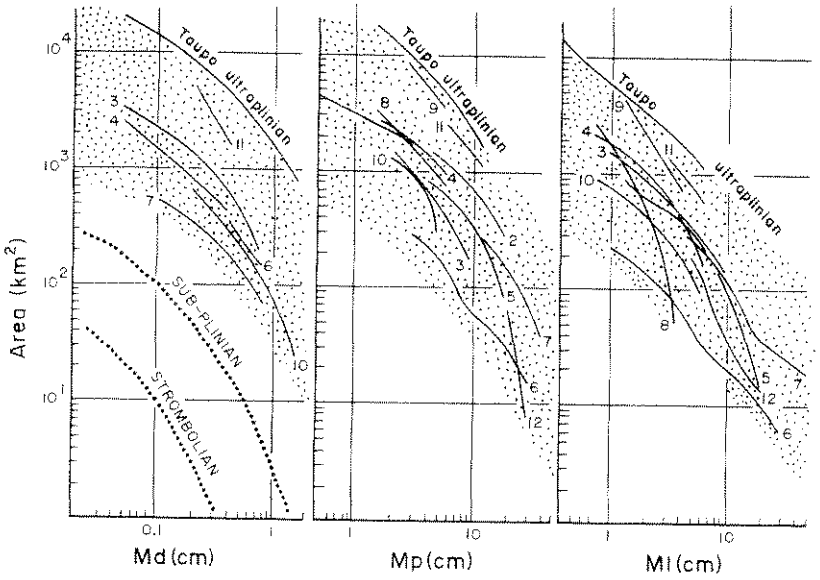

Figure 6.19 Plot of the area enclosed by isopleths of median grainsize (Md), maximum pumice diameter (Mp) and maximum lithic diameter (Ml). Stipple is field of plinian deposits. Deposits are labelled as in Figure 6.17 with the following additions: 9 Upper Bandelier, 10 La Primavera J, 11 Waimihia; 12 Minoan. (After G. P. L. Walker 1980, 1981b and Self & Wright *unpub. data* on the Bandelier plinian deposits.)

fragmentation level, which is the depth to the free surface of the magma where fragmentation is taking place (Fig. 3.4; and see L. Wilson 1980a for a detailed analysis). The theoretical models of L. Wilson (1980a) predict maximum plinian eruption velocities of 600 m s^{-1}, which would agree with maximum velocities deduced from the sizes of the largest ballistic clasts ejected in these eruptions. These exit velocities indicate that the volumetric discharge rates of magma can be as high as 10^6 m^3 s^{-1} (dense rock equivalent), which are substantially greater than in observed historic eruptions (Table 6.3). A continuous gas blast can probably not be sustained for a long time, and from the available data typical durations vary from one hour to one day (Table 6.4). The 1563 Fogo eruption lasted up to about two days overall, but its plinian eruption phase was interrupted during this time, and the deposits contain interbedded small ignimbrite flow units and other layers. The duration of large ignimbrite-forming eruptions which sometimes follow an initial plinian phase can be much longer (Ch. 8).

Table 6.3 Estimated muzzle velocities and volumetric eruption rates of some plinian eruptions.

Eruption	Maximum muzzle velocity ($m\ s^{-1}$)	Average volumetric eruption rate ($m^3\ s^{-1}$)
Upper Toluca	500	4.4×10^4
Minoan	330	2.8×10^4
Vesuvius AD 79	>225	1.6×10^4
Askja 1875	380	8.5×10^3
Fogo 1563	415	1.8×10^5
Santá Maria 1902	>270	1.2×10^5

Volumetric eruption rates are given in terms of dense rock equivalent.

Data from Bloomfield *et al.* (1977), Sparks *et al.* (1981), L. Wilson (1976, 1978, 1980b), G. P. L. Walker (1981b), S. N. Williams and Self (1983).

Table 6.4 Estimated durations of some plinian eruptions.

Eruption	Duration (h)	Source
Upper Toluca (11 600 years BP)	20–30	theoretical analysis
Minoan 1470 BC	20–40	theoretical analysis
Vesuvius AD 79	~24	historical records
Fogo 1563	~48	historical records
Askja 1875	6.5	historical records
Hekla 1947	1	observation
Mt St Helens 1980	9	observation

Data taken from Bloomfield *et al.* (1977), Sparks *et al.* (1981), L. Wilson (1976, 1978, 1980b).

As a plinian eruption proceeds, we can predict that two things will generally happen with time:

(a) deeper, and more gas-depleted, levels of the magma chamber will be tapped and

(b) widening of the vent by wall erosion will occur.

The effect of (a) is to reduce the gas velocity of the eruption column with time. The effect of (b) is to increase the mass discharge rate with time, and this will produce a column that steadily grows in height. Both (a) and (b) cause the effective density of a plinian column to increase steadily. This can continue until at some stage the density of the column becomes greater than that of the atmosphere, when gravitational collapse will occur to generate ignimbrite-forming pyroclastic flows. Models have shown that various combinations of magmatic gas content, gas velocity and vent radius produce convecting columns and others produce collapsing columns (L. Wilson 1976, Sparks & L. Wilson 1976, Sparks *et al.* 1978, L. Wilson *et al.* 1980; Fig. 6.20), and from these we can therefore predict when eruption column collapse will occur. Columns formed from magmas with high gas contents (>5 wt% water) are likely to show convective motion, whereas those with low gas contents (<1 wt% water) will form collapsing columns. In magmas with intermediate gas contents, collapse will occur when the vent radius exceeds a value defined in Figure 6.20. However, not all plinian eruptions continue to the collapse or ignimbrite-forming stage, and there are many examples of plinian deposits without associated ignimbrites – e.g. the 1875 Askja plinian deposit (Sparks *et al.* 1981), the 1902 Santa Maria deposit (S. N. Williams & Self 1983) and the Upper Toluca plinian deposit in Figure 6.13d.

With this theoretical background, we can now explain two common features of plinian fall deposits that have been described: reverse grading, and stratification in the upper parts of deposits. The models of L. Wilson *et al.* (1980) suggest that the major cause of reverse grading in plinian-fall deposits is vent-widening by wall erosion during the eruption. As an eruption continues and the vent widens, the mass discharge rate increases and, because of the increase in mass and energy flux, increased convective velocities will raise the height of the eruption column. Particles of a given size will be taken to increasing heights in the column before being released. d will then be transported downwind from the vent during the eruption. The increased proportion of larger clasts downwind with time will build up a reversely graded deposit. Shifts in the wind direction or speed could also have this effect, but these variables should also produce just as many examples of normally graded plinian fall deposits. This is therefore not a general mechanism to explain the common occurrence of reverse grading in many deposits. Local reverse grading could also be found in falls deposited in water, or on very steep slopes followed by secondary mass (grain) flow (see Duffield *et al.* 1979).

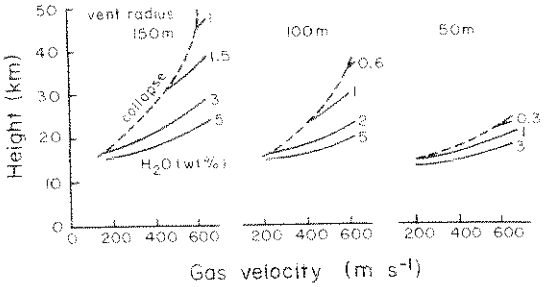

Figure 6.20 Eruption column height as a function of the muzzle gas velocity for three different vent radii. In each case curves are given for constant values of magmatic water content. Column collapse occurs for combinations of values to the left of the broken line. (After L. Wilson 1976.)

Widening of the vent, together with an increased rate of erosion during the eruption, also explains why many plinian fall deposits show a vertical increase in the proportion of accessory lithics. An estimate of the lithic content therefore indicates the amount of wall erosion and the size of conduit. For example, the Fogo A plinian pumice deposit on São Miguel contains 0.09 km^3 of lithic fragments (14 wt%), and if the magma source was at a depth of 5 km this would be equivalent to a hypothetical cored-out cylindrical conduit of diameter 78 m. However, erosion is likely to be more important near the surface, where rocks are weak and less consolidated, and flaring of the vent is therefore probably likely (L. Wilson *et al.* 1980).

The explanation of the stratification observed at the tops of many plinian deposits seems to be that it is caused by instabilities in a column nearing the point of collapse. Changes in wind direction and

speed could cause stratified layers, but their common occurrence at this level, and the presence of interbedded pyroclastic flows and surges, suggests a more general mechanism, as with reverse grading. Any changes in gas velocity or mass discharge rate in a column verging on collapse will have pronounced effects on its behaviour. Small collapse events that generate pyroclastic flows and surges may occur, for instance, with a sudden increase in mass discharge rate. A convective column could then be re-established with a slight increase in gas velocity due to a small increase in gas content of the magma. Choking of the vent by collapse of the walls will also reduce mass discharge rate, re-establishing a convecting column, but after this lithic debris has been removed by ejection the wider vent will promote collapse of the column. A complex sequence of activity and of pyroclastic deposits could therefore be generated before massive collapse of the whole column occurs, leading to a major ignimbrite-forming eruption.

6.5 Sub-plinian

These are pumice-fall deposits which resemble plinian deposits in the field, especially near the vent, but when mapped out have a smaller dispersal and are small volumetrically. G. P. L. Walker (1973b) set arbitrary D limits for them of between 5 and 500 km^2 (Fig. 6.2). They are a common type of pyroclastic fall deposit, although only a few specific descriptions occur in the literature. This is because studies of pumice fall deposits have generally concentrated on the larger, more-dramatic examples which are usually plinian in their F and D characteristics. However, Self (1976) described a number of sub-plinian fall deposits on Terceira in the Azores (e.g. Fig. 6.21) and Booth *et al.* (1978) documented examples on São Miguel. Sub-plinian pyroclastic fall deposits are a product of rhyolite volcanoes and stratovolcanoes, like their larger plinian counterparts. Many form during an early explosive phase accompanying the effusion of a small rhyolite dome or coulée, as do the examples on Terceira. However, plinian deposits can also be erupted in this situation.

Sub-plinian eruptions are scaled-down plinian eruptions, and their mechanisms and dynamics can be treated as essentially the same (L. Wilson 1976, 1980b). Large lithics indicate that in some eruptions muzzle velocities are as high as in some plinian events (>400 m s^{-1}), although the lower range is 100 m s^{-1} (L. Wilson 1976). Mass discharge rate is likely to be lower for sub-plinian events, and this is the main factor controlling eruption column height and dispersal. The sub-plinian pumice-fall deposits on Terceira are well-stratified and Self (1976) suggested that there were large fluctuations in the gas exit velocity, and hence mass discharge rate. This would also inhibit the development of a fully maintained convective plume, which would therefore not attain the heights associated with plinian columns. Sub-plinian eruptions can lead to the generation of ignimbrite-forming pyroclastic flows similar to the larger plinian ones. The examples mentioned above from the Azores do not show this eruption sequence. However, it is shown in the eruption of Krakatau in 1883. A pumice-fall deposit which preceded an ignimbrite erupted at Krakatau is sub-plinian rather than plinian in its characteristics (Self & Rampino 1981).

A number of basaltic or near-basaltic scoria fall deposits are now also known to be sub-plinian in their dispersal characteristics, rather than strombolian. G. P. L. Walker (1973b) cites as an example the 1970 Hekla eruption, and another example is the scoria-fall deposit erupted with the formation of Sunset Crater (AD 1065) in the San Francisco volcanic field, Arizona (Amos *et al.* 1981; Fig. 6.11 & Plate 5). As well as producing a very widely dispersed scoria-fall deposit (dense rock equivalent, DRE = 0.30 km^3) the Sunset Crater eruption also built a scoria cone 300 m high (DRE = 0.15 km^3), and in this respect is more typically strombolian in its character. For such widely dispersed scoria-fall deposits, one has to envisage a fully maintained convective plume which reached greater heights than in normal strombolian eruptions. The gas thrust part of the column in the Sunset Crater eruption may have reached heights of several hundred metres, rather than the 50–200 m that is usual in normal strombolian eruptions (Amos *et al.* 1981). Such energetic basaltic eruption columns

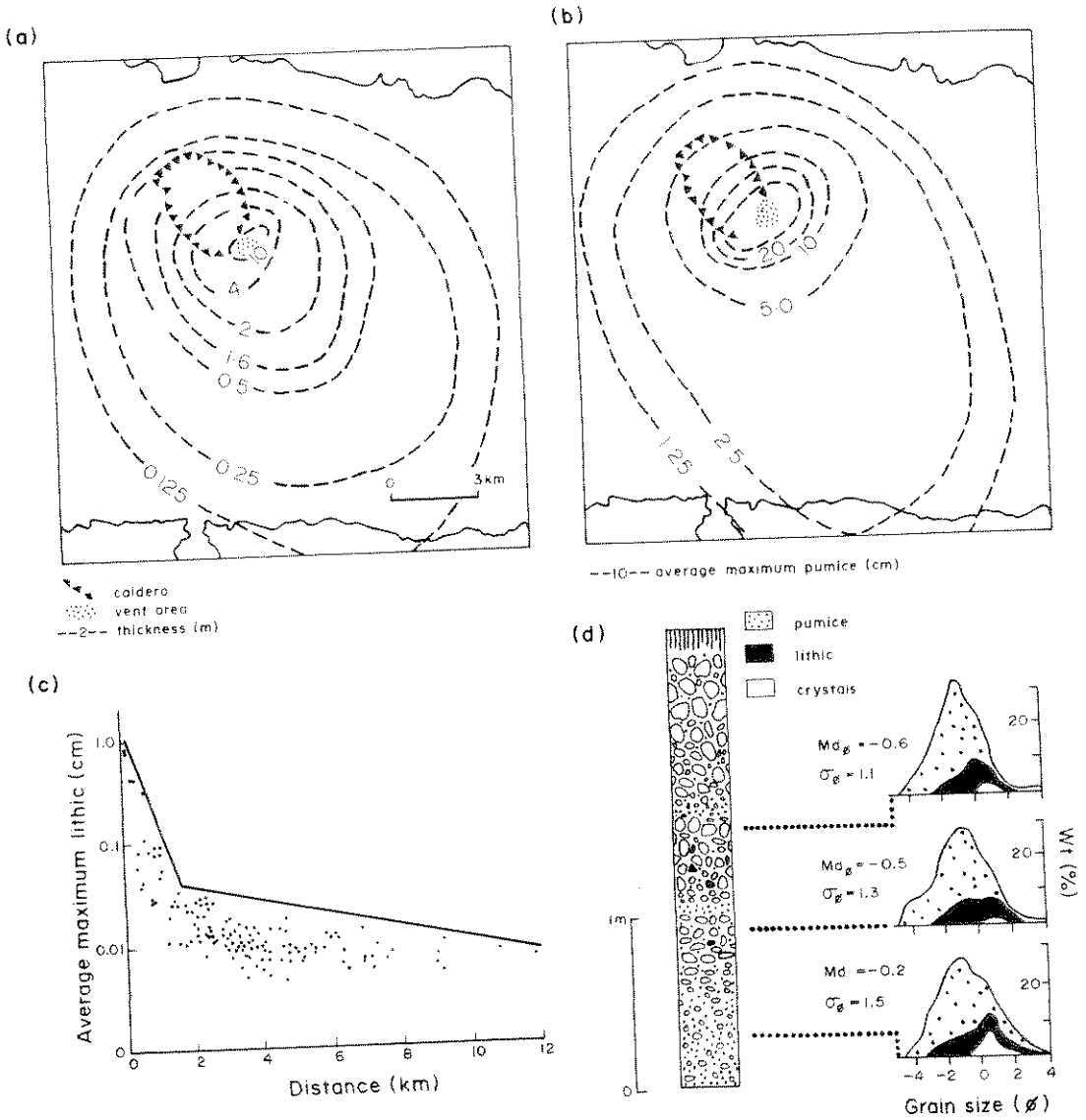

Figure 6.21 Sub-plinian pumice fall deposit from Terceira, Azores. (a) Isopach map giving thickness in metres. (b) Averag maximum diameter of three largest pumice fragments in centimetres. (c) Average maximum diameter of three largest lith fragments against distance from source. (d) Section 1.8 km SE of source on dispersal axis. Frequency curves of weig percentage against grainsize show proportions of pumice, crystals and lithics for three sieved samples, together with vertic variation in σ_ϕ and Md. (After Self 1976.)

(which in some examples are also known to have attained plinian proportions, see earlier) may have formed through a combination of a relatively high magma discharge rate and high initial magmatic gas contents.

6.6 Ultraplinian

'Ultraplinian' has been recently introduced as separate type by G. P. L. Walker (1980) to descr the most widely dispersed plinian fall depos

Published data are as yet only available for one deposit, the Taupo pumice, which forms part of the eruption sequence of the AD 186 eruption of Lake Taupo, New Zealand. The products of this eruption will be discussed in more detail in Chapter 8.

The Taupo pumice is currently the most widely dispersed pyroclastic fall deposit known. *D*- and *F*-values are much higher than for normal plinian deposits (Fig. 6.2) and clasts are dispersed over a much wider area (Figs 6.17–19). The Taupo pumice only has a maximum measured thickness of 1.8 m which, by comparison with most near-vent plinian deposits, is rather thin. Another feature is that the deposit is very enriched in free crystals. This results from the high degree of fragmentation, and from the loss of a large proportion of vitric material by aeolian fractionation. Data from crystal concentration studies on the Taupo pumice show that 80%, mainly glass, fell out to sea further than 220 km from the vent.

Because of the great column height, which is estimated to be >50 km (G. P. L. Walker 1980), the deposit is also thickest 20 km downwind from the vent. Thus in these situations the isopach map must be used with caution as an indication of the vent position. From other evidence, the vent for this eruption is known to be in Lake Taupo.

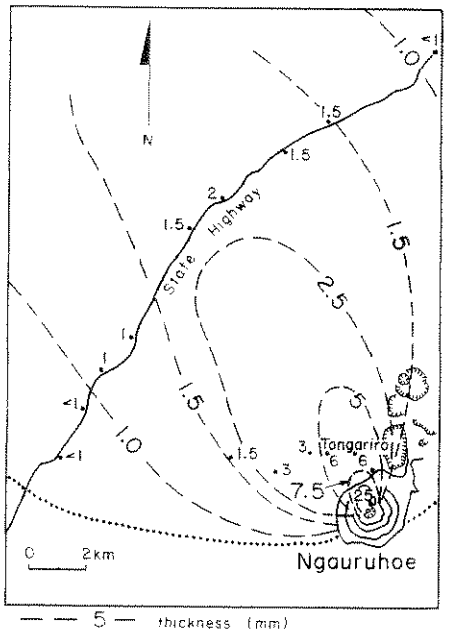

Figure 6.22 Isopach map of the vulcanian pyroclastic fall deposit erupted from Ngauruhoe on 28–29 March 1974. Note thicknesses are in millimetres. (After Self 1974.)

6.7 Vulcanian

Vulcanian pyroclastic fall deposits from individual eruptions are thin, small volume (<1 km^3), stratified ash deposits which contain large ballistic bombs and blocks near to the vent, sometimes with breadcrusted and jointed surfaces (Figs 6.22–24). In composition they are usually intermediate (basaltic-andesite, andesite, dacite). They are common products of andesite and basaltic-andesite stratovolcanoes. However, they are usually so thin and fine-grained that they are soon eroded by wind and water. When eruptions continue for a few years, bedded sequences can be built up near the vent, but these are never likely to be of great thickness, e.g. less than 2 m of ash-fall deposits accumulated just 800 m downwind of the vent on Irazú volcano, Costa Rica, from the eruptions between March 1963 and mid-1964 (Fig. 6.23).

Vulcanian activity has been observed in a large number of historic eruptions: for example; Fuego

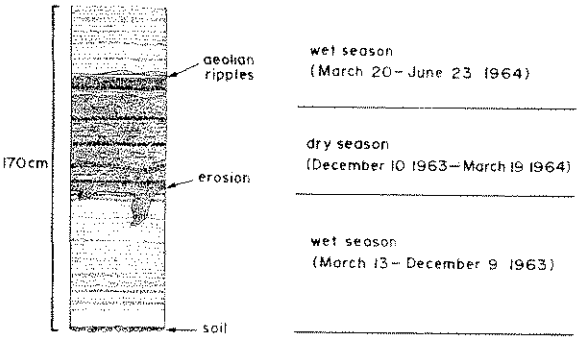

Figure 6.23 Section, dug 23 June 1964, through ash deposits accumulated from vulcanian activity at Irazú, Costa Rica, which began 13 March 1963. The location is just 800 m downwind of the vent. While many of the ash layers are the deposits of single ash falls, others represent layering produced mechanically by falling raindrops, sheet wash and aeolian reworking. For this reason ash deposited during the wet seasons appears to be better stratified. The prominent erosion surface results from a huge downpour on 10 December 1963. (After Murata *et al.* 1966.)

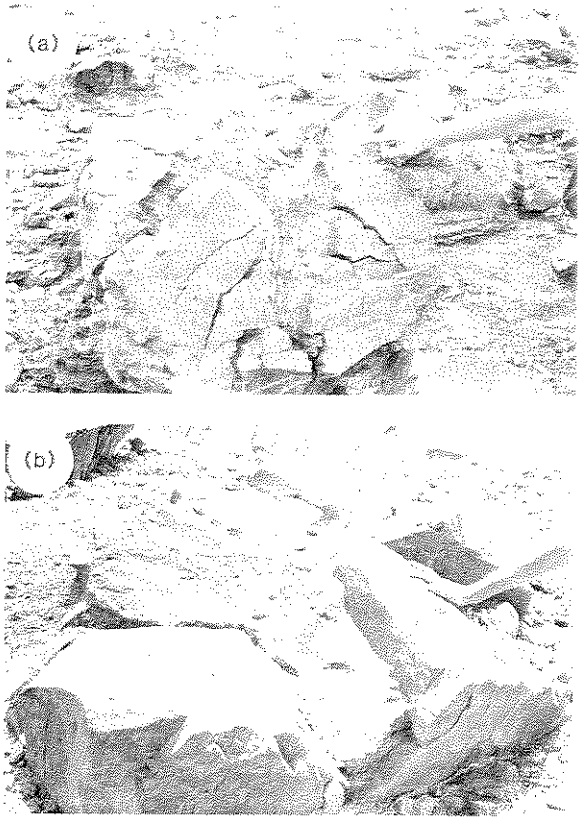

Figure 6.24 Ballistic blocks from the 1888–90 eruption of Vulcano. (a) Breadcrusted block. (b) Block having internal radial cooling joints.

volcano, Guatemala, which has had 25 vulcanian eruptions since 1944 (Rose *et al.* 1978, Martin & Rose 1981); the 1888–90 eruptions of Vulcano in the Aeolian Islands, which are the 'type example' of this activity (MacDonald 1972); the Irazú eruption (Murata *et al.* 1966); the 1976 eruption of Augustine volcano, Alaska (Kienle & Shaw 1979); and examples shown in Figure 6.25.

Activity during vulcanian eruptions proceeds as a number of discrete cannon-like explosions at intervals of commonly tens of minutes to hours. These short-lived explosions produce a series of small eruption columns (<5 to 10 km) with plumes strung out downwind of the volcano. Pyroclastic fall deposits are fine-grained with a wide dispersal (Fig. 6.25). Larger fragments in the column simply fall back around or into the vent, to be further fragmented and abraded. Commonly, a large part

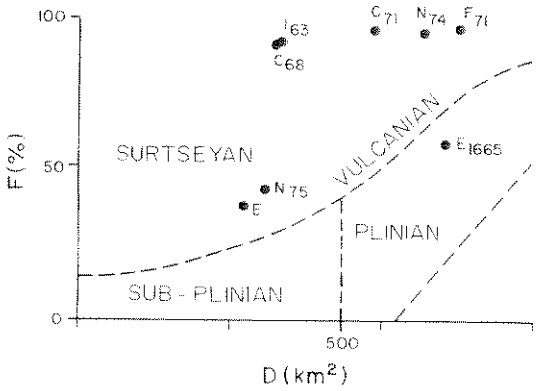

Figure 6.25 *D–F* plot showing the field of vulcanian deposits: C_{68} and C_{71}, eruptions of Cerro Negro, Guatemala, in 1968 and 1971; E, an old undated fall deposit of Mt Egmont, New Zealand; E_{1665}, fall deposit of the 1665 eruption of Mt Egmont; F_{71}, eruption of Fuego in 1971; I_{63}, eruption of Irazu in 1963; N_{74} and N_{75}, eruptions of Ngauruhoe in 1974 and 1975. (After J. V. Wright *et al.* 1980.)

of the material ejected with each explosion is not juvenile, but includes a large fraction of country rock as accessory lithics. At the onset of an eruption a plug of older, pre-existing lava may first be exploded out. However, during recently observed eruptions (for example, Fuego in 1974 and Ngauruhoe in 1975) coarser-grained scoria-fall deposits of more limited dispersal were produced during periods of more-intense, maintained explosions

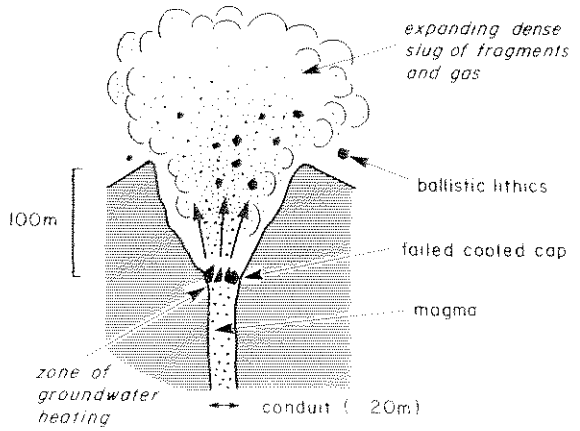

Figure 6.26 Schematic cross section through the crater of a stratovolcano at the time of a vulcanian explosion. Expanding 'cauliflower'-shaped slug rapidly decelerates during this gas thrust phase. (After Self *et al.* 1979.)

with continuous gas-streaming. Eruption columns reached heights of >10 to 20 km. This type of activity occurs intermittently with periods of short-lived explosions, and hence two types of fall deposit are formed during eruptions which have overall been termed vulcanian. The coarser scoria fall deposits seem to have similar fragmentation and dispersal indices to those deposits termed violent strombolian by G. P. L. Walker (1973b).

Small-volume pyroclastic flows are also frequently generated during vulcanian eruptions when large amounts of ejecta fall back around the vent. Very good descriptions of scoria flows associated with the 1974 Fuego and 1975 Ngauruhoe eruptions are given, respectively, by D. K. Davies *et al.* (1978a) and Nairn and Self (1978) (Fig. 6.26 and see Ch. 5). However, not all vulcanian eruptions produce pyroclastic flows, e.g. Irazú (1963–5).

The mechanisms and dynamics of vulcanian explosions have most recently been described by Schmincke (1977), Nairn and Self (1978), Self *et al.* (1979) and L. Wilson (1980a). Self *et al.* (1979) and L. Wilson (1980a) have critically evaluated the energy equations used in previous studies for the analysis of this type of explosion (e.g. Minakami 1950, Fudali & Melson 1972, McBirney 1973). Transient explosions, typical of vulcanian eruptions, result from the sudden release of pressure in a gas due to the failure of some cap rock (Self *et al.* 1979, L. Wilson 1980a; Fig. 6.26). Because of the pressures involved, this cap rock is unlikely to be simply a layer of unconsolidated clasts. It is most

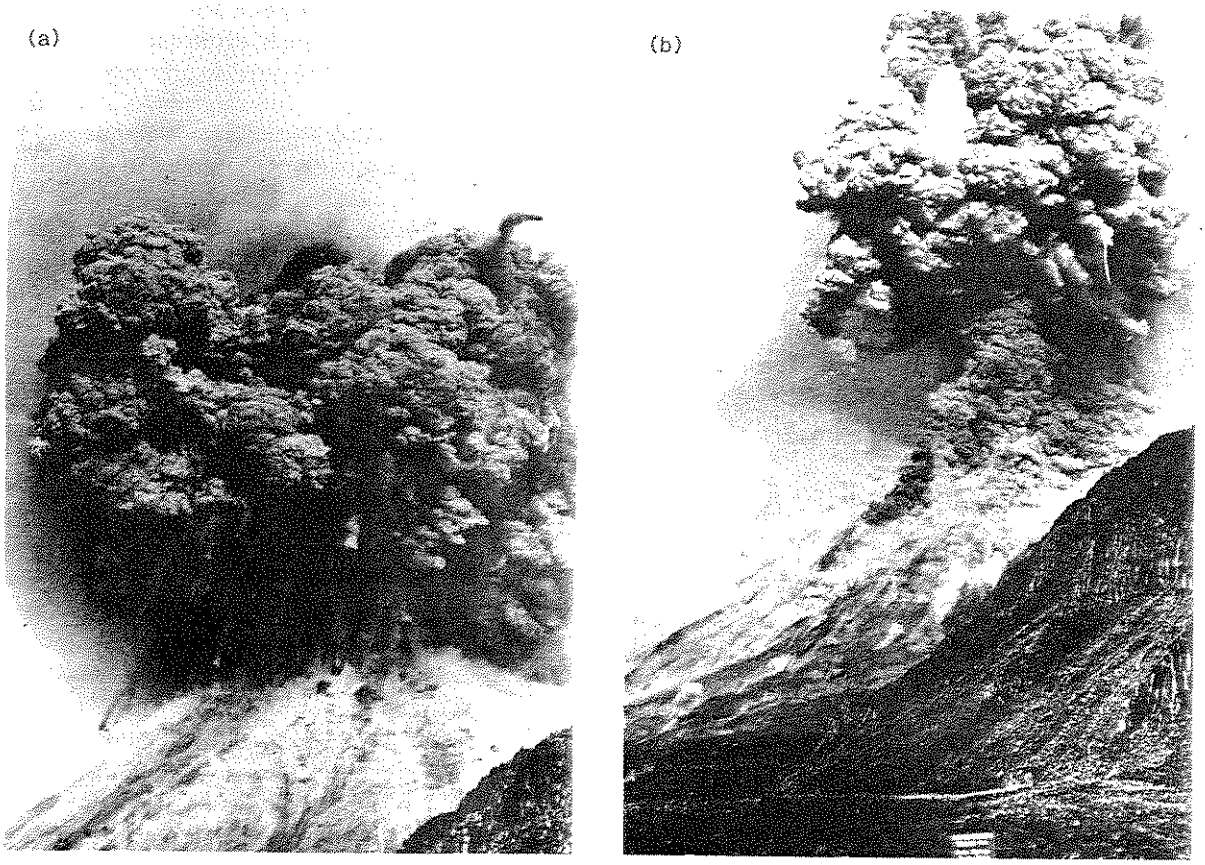

Figure 6.27 Eruption of Ngauruhoe, New Zealand, at 18.10 h on 19 February 1975. (a) Expanding slug at +8 s; large blocks are 20–30 m in diameter and breaking up with dust trails. (b) Collapse of dense interior of slug to form pyroclastic flows with air-fall plume rising above summit at +45 s. (After Nairn & Self 1978.)

likely to be the cooled, congealed cap of new magma that has risen after the previous explosion, or it could be an older plug. The pressure rise may be due to exsolution of magmatic gas, or to the heating and partial vaporisation of ground water, but not to violent mixing as in a phreatomagmatic eruption.

Gas pressure builds up until the overlying cap fails, in tension or shear. For rocks at temperatures up to 950°C, pressures of up to a few hundred bars are expected (L. Wilson 1980a). An explosion releases a vertical slug of fragments and gas, with initial velocities that may be supersonic, in which case a shock wave would also be propagated (Nairn 1976). The history of one explosion from the Ngauruhoe 1975 eruption shown in Figure 6.27 is documented in Figure 6.28. The slug of material was ejected at an estimated initial velocity of ~400 m s^{-1}, and partial collapse of the column occurred at nearly 500 m above the crater rim to generate a pyroclastic flow (Fig. 6.27b).

Self *et al.* (1979) and L. Wilson (1980a) have estimated maximum velocities of ejected debris in vulcanian explosions as a function of the pressure beneath the retaining plug at the time it fails. Their calculations suggest that previous estimates of pre-explosion gas pressures (of the order of a few kilobars) are overestimated by an order of magnitude. They also indicate that initial velocities up to 200 m s^{-1} are readily explicable by magmatic gas contents (up to a few weight per cent), and pressures up to a few hundred bars are probably consistent with material strengths. However, for initial velocities above 300 m s^{-1} the influence of external water must be postulated; even if pressures of several kilobars (which cannot be supported by rock strengths) are assumed, unreasonable magmatic water content of >10 wt% is implied. Heated ground water is probably a significant feature in such explosions, but not necessarily an essential feature as proposed by Schmincke (1977).

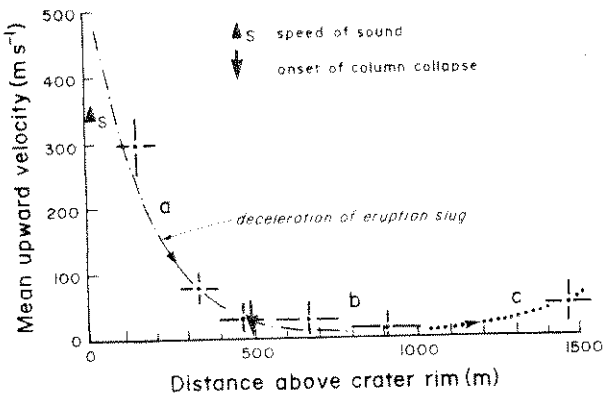

Figure 6.28 History of the 18.10 h vulcanian explosion at Ngauruhoe, New Zealand, on 19 February 1975. Data are from the analysis of still photographs; errors are shown as bars. Curved line approximates exponential deceleration of the eruption slug. The steep part of the curve (a) represents deceleration in the gas thrust phase, the flat portion (b) represents a slow, stable velocity condition while mixing with air and column collapse took place; part (c) shows a slight increase in velocity as convective recovery and rise of the plume began. This event ejected 2×10^6 kg of rock, although only half of this was juvenile. Half of the total volume then collapsed to form the pyroclastic flow. (After Self *et al.* 1979.)

6.8 Surtseyan and phreatoplinian

These terms are used to describe pyroclastic fall deposits resulting from eruptions which have taken place in the sea or a lake, or by contact with ground water. Such eruptions are most generally called phreatomagmatic or hydrovolcanic (Chs 3 & 5). Both types of deposit have extreme fragmentation, F being nearly 100% (Fig. 6.2), and this results from the magma–water interaction. Surtseyan pyroclastic fall deposits have moderate dispersal, while phreatoplinian deposits can be extremely widely dispersed (Fig. 6.2).

There is a tendency to associate specific magma compositions with each of these two types of deposit, based on the compositions of the type examples used to define the terms originally (basaltic for surtseyan, rhyolitic for phreatoplinian; see below). However, given the right conditions, the eruption of any magma type may produce the dispersal and fragmentation characteristics defining these two types of deposits on a D–F plot. It may thus be possible to find rhyolitic surtseyan deposits, and andesitic, trachytic and even basaltic phreatoplinian deposits.

6.8.1 SURTSEYAN ACTIVITY AND DEPOSITS

The term 'surtseyan' was used by G. P. L. Walker (1973b) to describe the type of air-fall deposit which would result from similar activity to that observed during the eruption of Surtsey in 1963. Since then, the surtseyan field has been used in a general way to group basaltic fall deposits resulting from different types of hydrovolcanic activity. Kokelaar (1983) pointed out that there may be significant differences between true surtseyan activity, where (sea) water floods into the top of an open vent, and *true* phreatomagmatic activity, involving trapped ground water. However, there is still much to be learnt about such explosive interactions, and for our purposes it is convenient to continue to use 'surtseyan' for the pyroclastic fall field on *D–F* plots irrespective of the environment of magma–water interaction or vent conditions, and 'phreatomagmatic' more loosely for all types of hydrovolcanic activity. This unfortunately still leaves unresolved problems. For instance, we use the basaltic-andesite ash fall deposited during the 1979 eruption of Soufrière, St Vincent, as an example of surtseyan activity because of its well documented phreatomagmatic characteristics and moderate dispersal. However, in detail, the high concentration of lithics is not consistent with a true surtseyan ash fall, and the deposit does not fit easily into a *D–F* pigeonhole. Perhaps classification as (phreatomagmatic) vulcanian would be better (R. S. J. Sparks, *pers. comm.*). Future studies may clarify the grainsize and dispersal characteristics produced during different types of hydrovolcanic eruption, and may lead to the definition of separate fields on the *D–F* diagram.

Phreatomagmatic activity is very common in basaltic volcanic fields, producing maars, tuff rings and tuff cones (Ch. 13). These constructional forms are largely built up from the deposits of base surges (Ch. 5), and thin ash-fall beds occur downwind (Fig. 6.29). Several examples of this type of eruption have occurred this century (Section 5.6). Eruptions of basic to intermediate magmas through small crater lakes on some stratovolcanoes have also produced phreatomagmatic air-fall deposits which

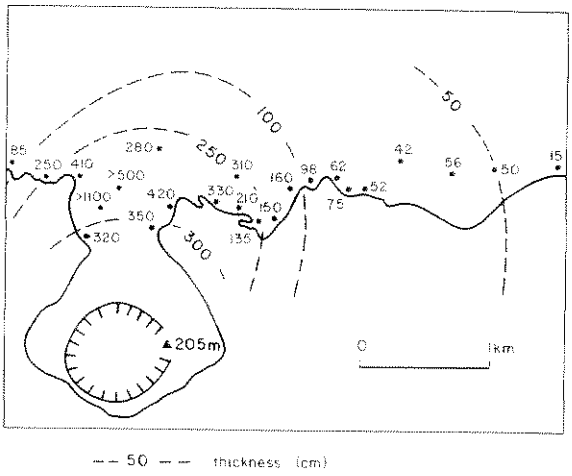

Figure 6.29 Isopach map of the surtseyan ash-fall deposit from the Monte Brazil tuff ring on Terceira. (After Self 1976.)

would have to be included under our broad definition (e.g. the 1979 eruption of Soufrière, St Vincent, Shepherd & Sigurdsson 1982; Fig. 6.30).

The downwind air-fall deposits are thin, fine-grained ashes (Figs 6.29–32), and internally they may be well laminated (Fig. 6.32) because phreatomagmatic activity seems to occur as a number of short explosions. They often contain accretionary lapilli (Ch. 5), and SEM photographs of the ashes show very angular, broken surfaces due to the magma–water interaction (G. P. L. Walker & Croasdale 1972, Heiken 1974). For air-fall deposits they can be poorly sorted (Figs 6.30c & 31). Studies of the 1979 Soufrière air-fall ash layer have shown that bimodal sorting may be an important feature (Sigurdsson 1982, Brazier *et al.* 1982; Fig. 6.30c). Bimodality and poor sorting is attributed to premature fall-out of aggregated wet or damp ash in the eruption column or downwind plume. Accreted ash could occur as accretionary lapilli, or as unstructured ash clumps. During the 1979 Soufrière activity such ash clumps were observed to fall and then break on impact.

Nearer to the vent this type of air-fall deposit is found interbedded with base surge deposits. One problem in near-vent situations is distinguishing air-fall layers from planar-bedded base surge deposits, and we will suggest the criteria to discriminate between them in Chapter 7. In many cases,

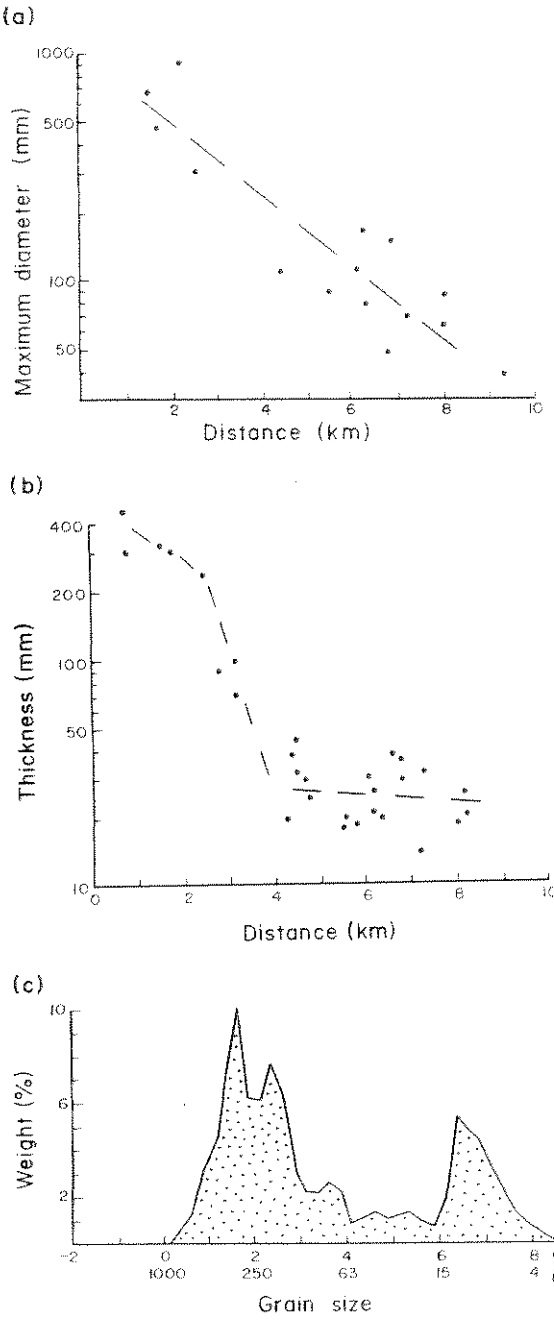

Figure 6.30 The phreatomagmatic ash fall deposit erupted in 1979 from Soufriere, St Vincent, Lesser Antilles. Variation in (a) maximum dense clast diameter and (b) thickness, both as a function of distance from vent. (c) Bimodal size distribution in a sample collected from the lower part of the deposit. (After Sigurdsson 1982.)

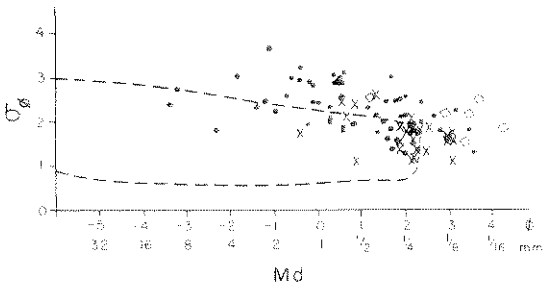

Figure 6.31 Md_ϕ/σ_ϕ for some surtseyan ash-fall deposits. Solid circles are samples collected at vent, while crosses are downwind deposits. Diamonds are ash-fall deposits from phreatomagmatic eruptions of the Quill, St Eustatius, Lesser Antilles; all of the samples were collected between 2 and 3 km from the vent. Broken line is the field of magmatic basaltic (strombolian) fall deposits (from Fig. 6.7). (After G. P. L. Walker & Croasdale 1972 and J. V. Wright *unpub. data* from St Eustatius.)

both modes of deposition may have occurred simultaneously as ash from a previous explosion, or maintained column, fell around the vent into newly generated surges. Other evidence of such ashes being wet may be entombed gas cavities (Ch. 5).

6.8.2 PHREATOPLINIAN ACTIVITY AND DEPOSITS

The term 'phreatoplinian' was introduced by Self and Sparks (1978) for the silicic analogue of surtseyan, and they described several examples, documenting in detail widespread ash layers from the Oruanui Formation (now redefined and described by Self (1983) as the Wairakei Formation), New Zealand, and from a phreatomagmatic phase of the 1875 Askja eruption (Figs 6.33–35). They also mention another example in New Zealand, the Rotongaio ash, and examples from the Minoan eruption of Santorini (Bond & Sparks 1976) and São Miguel (Booth *et al.* 1978). Self (1983) discussed the Oruanui (Wairakei) Formation in detail and G. P. L. Walker (1981a) documented the Rotongaio ash and the Hatepe ash, both of which were formed in phreatomagmatic episodes during the Taupo AD 186 eruption. We shall describe these deposits along with the ultraplinian deposit also produced by that eruption in Chapter 8. The Vesuvius AD 79 eruption also produced phreatoplinian layers, as was previously mentioned (Ch. 5).

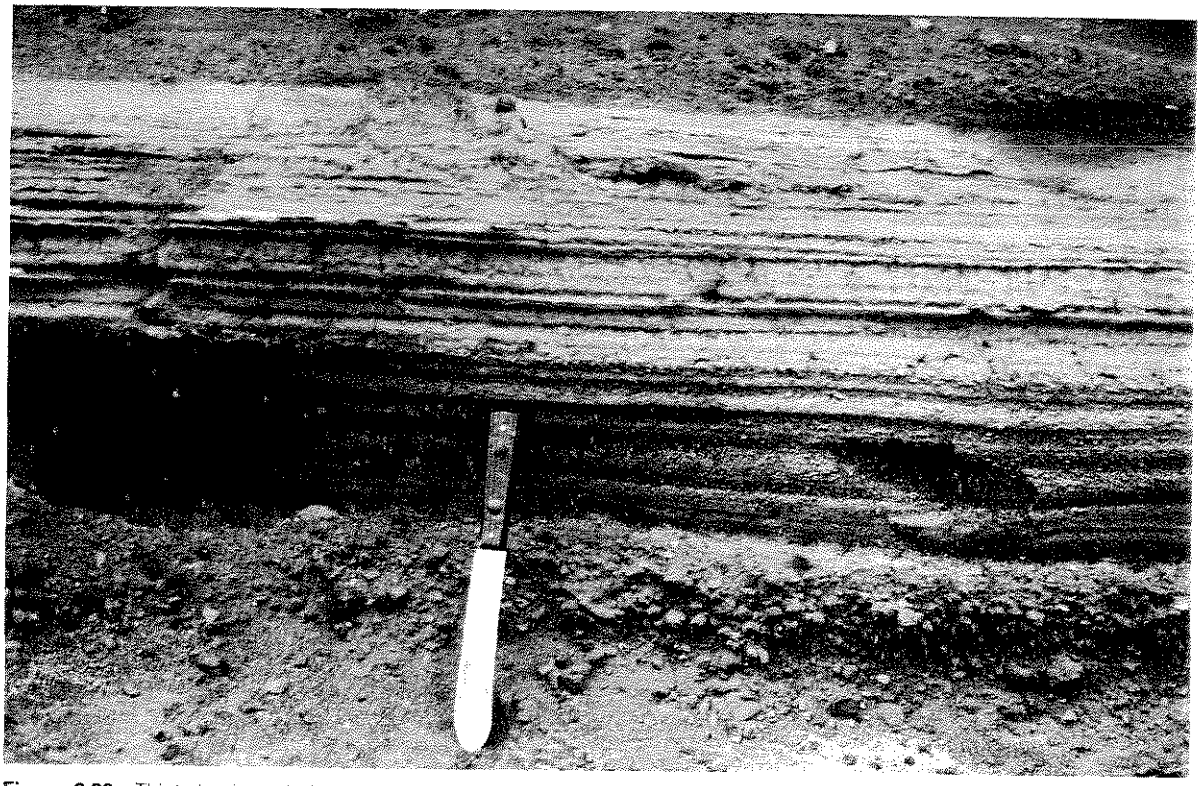

Figure 6.32 Thinly laminated phreatomagmatic ash-fall deposit of intermediate composition erupted from the stratovolcano Mt Misery on St Kitts, Lesser Antilles (see Fig. 13.28; this ash deposit also contains accretionary lapilli (not visible)). Knife is 30 cm long.

All of these phreatoplinian deposits were produced during phreatomagmatic phases of much larger rhyolitic eruptions which involved several different styles of activity. Collectively, these include plinian, base surge and ignimbrite-forming activity (Fig. 6.33). With the exception of the examples from Santorini and Vesuvius, they all involved eruption of rhyolitic magma through caldera lakes. In the Minoan eruption, sea water gained access to the vent on Santorini. During the Vesuvius AD 79 eruption, water from a deep aquifer is thought to have gained access to the magma chamber (Ch. 5).

The extremely wide dispersal of these deposits (Fig. 6.36) indicates a high eruption column (of plinian proportions), yet all of the other characteristics of the deposits indicate that they have a phreatomagmatic origin. Deposits are very fine-grained, even close to source (Fig. 6.35) and accretionary lapilli are common. They may be finely laminated, especially towards the vent, and near to the vent they are often associated with base surge deposits (Fig. 6.33). Deposits are poorly sorted for pyroclastic falls, especially considering their median grainsize, and their size distributions are bimodal or strongly negatively skewed, or both, indicating that they have an extended coarse tail (Fig. 6.37). In contrast, plinian deposits are positively skewed. SEM studies show that blocky shards are typical (Heiken 1972, 1974, Wohletz 1983; Ch. 3), although the phreatoplinian deposits of the Askja 1875 eruption do contain 'vesiculated' cuspate shards (Sparks *et al.* 1981), more usually associated with magmatic eruptions, as do the deposits of the Oruanui Formation (Self 1983).

Laterally, phreatoplinian deposits become imperceptibly thin and fine over wide areas. Downwind there is little sorting of the size distribution,

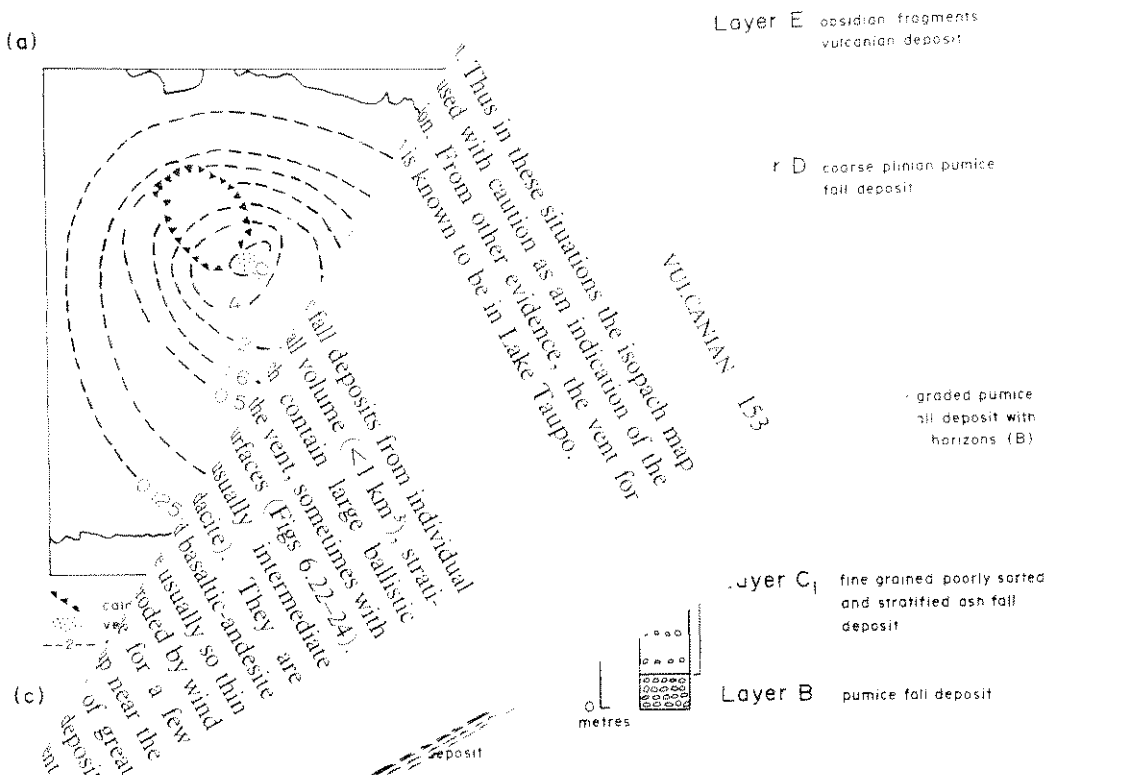

'Thus in these situations the isopach map used with caution as an indication of the ...on. From other evidence, the vent for ...is known to be in Lake Taupo.

VULCANIAN 153

...fall deposits from individual ...all volume (<1 km³), strati... ...ds contain large ballistic ...the vent, sometimes with ...surfaces (Figs 6.22–24). ...usually intermediate ...dacite). They are ...(basaltic-andesite ...usually so thin ...voded by wind ...for a few ...p near the ...of great ...deposits ...ent on ...ions.

...through the deposits of two eruptions which produced phreatoplinian ...Taraken Formation, New Zealand, reconstructed close to source north of Lake ...basal members (1–3) are exaggerated; 'e' indicates erosional breaks that occurred ...(b) The products of the Askja eruption, Iceland on 28–29 March 1875. (After Self &

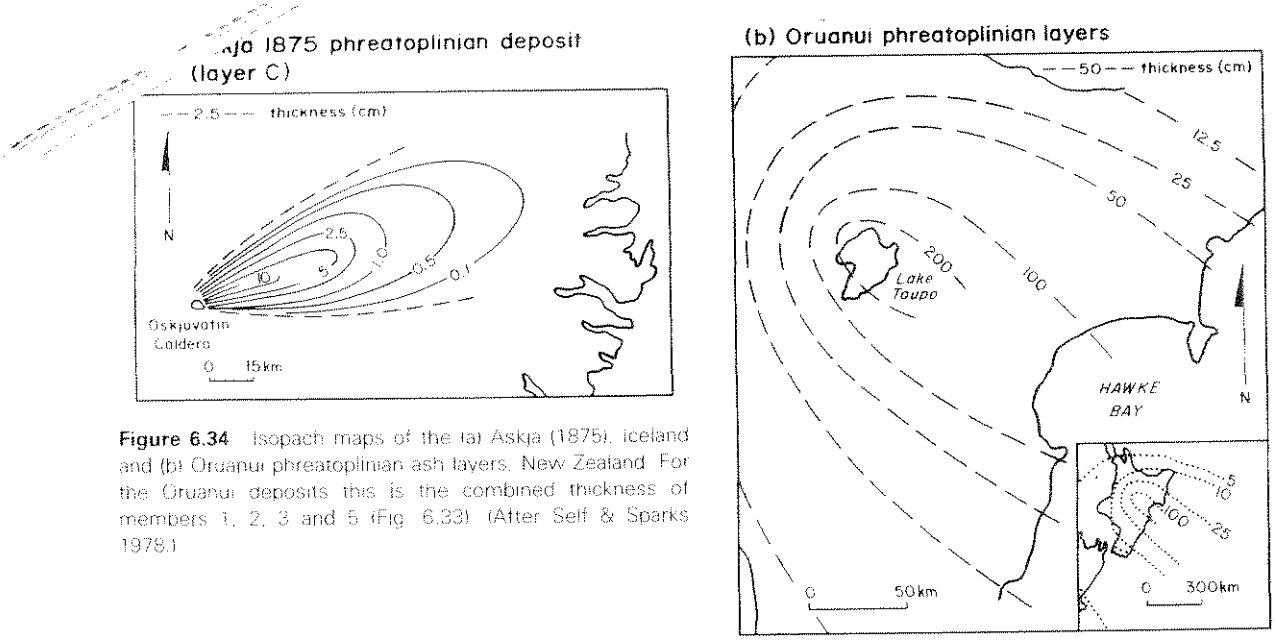

Figure 6.34 Isopach maps of the (a) Askja (1875), Iceland and (b) Oruanui phreatoplinian ash layers, New Zealand. For the Oruanui deposits this is the combined thickness of members 1, 2, 3 and 5 (Fig. 6.33). (After Self & Sparks 1978.)

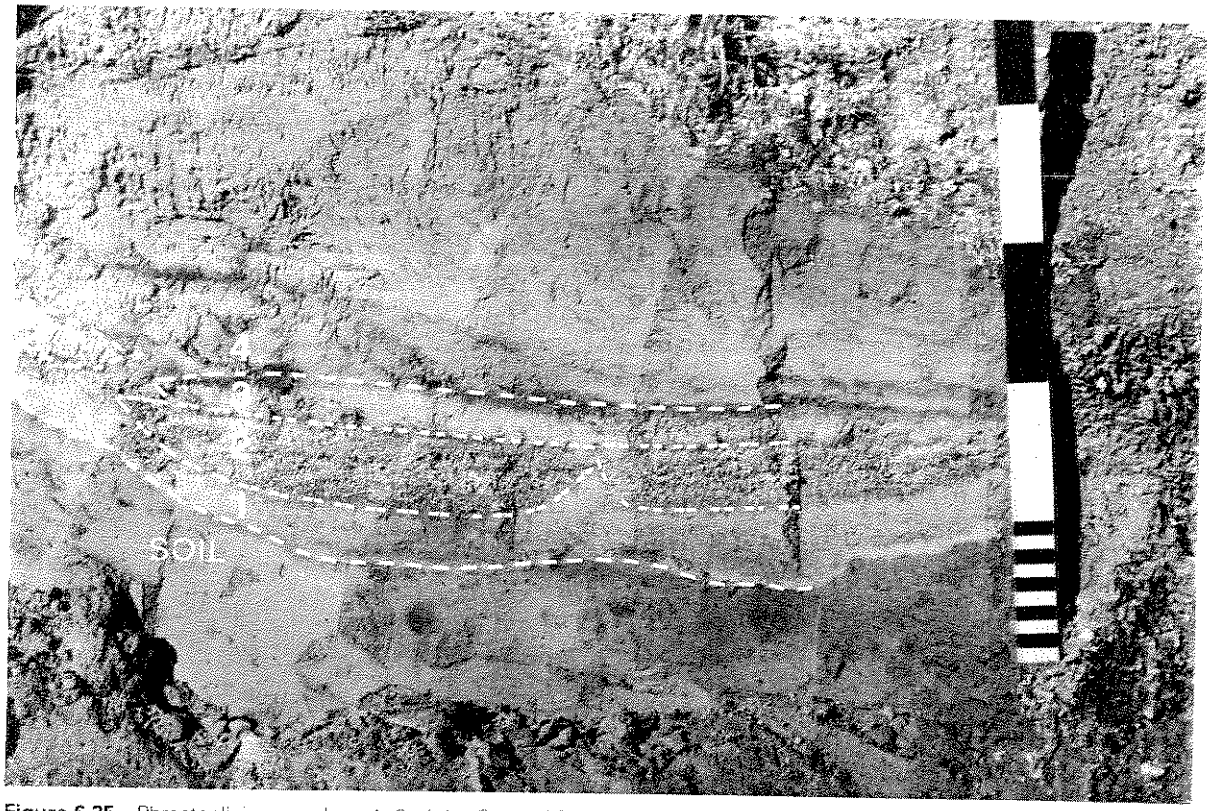

Figure 6.35 Phreatoplinian members 1–3 of the Oruanui Formation, New Zealand, 25 km from source. Member 4 is the base of the co-eruptive Oruanui ignimbrite. Erosion surfaces between members can be seen. The scale is 45 cm long. (After Self & Sparks 1978.)

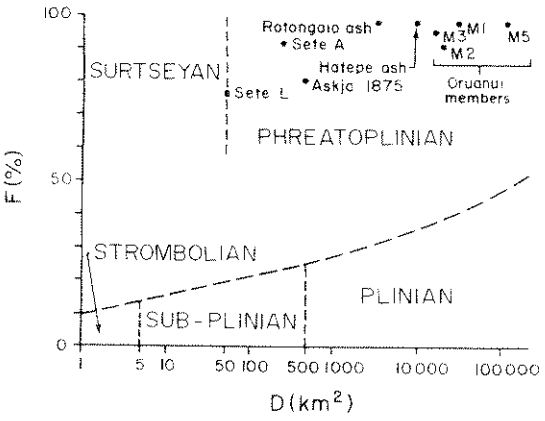

Figure 6.36 *D–F* plot of phreatoplinian deposits. (After Self & Sparks 1978 and G. P. L. Walker 1981a.)

and it is only the larger particles that are lost with increasing distance from the vent. This type of grading is *coarse-tail grading*, and contrasts with the distribution grading typical of plinian deposits where, laterally, sorting affects the whole size distribution (Fig. 6.37). Downwind sorting of fines must be inhibited in some way, and involves the bringing down of different-sized particles in aggregates or clumps to explain why these deposits are so fine-grained near source and so poorly sorted. These could fall as accretionary lapilli, but perhaps in many cases as unstructured clumps of ash. More extreme would be the wholesale water-flushing of the downwind plume, in which case ash could fall as 'mud-rain'. G. P. L. Walker (1981d) described a type of microbedding attributed to the splashing of falling water during deposition of the Hatepe ash. The source of most of the water was likely to have

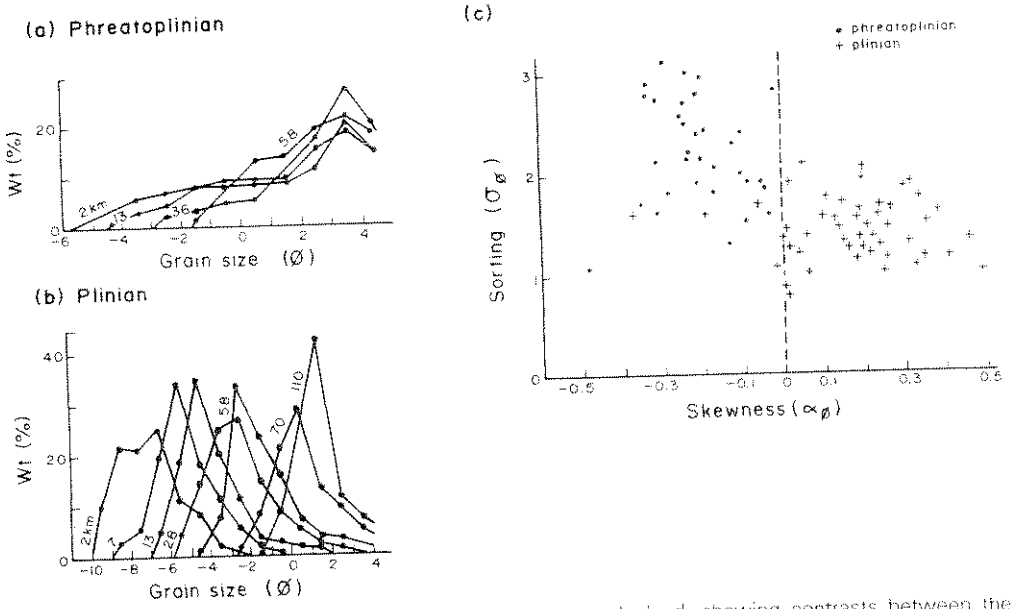

Figure 6.37 Grainsize data from the 1875 Askja deposits, Iceland, showing contrasts between the (a) phreatoplinian (layer C) and (b) plinian (layer D) deposits (Fig. 6.33). Frequency-grainsize curves are for samples collected at various distances downwind. (c) Plot of skewness against sorting. (After Sparks *et al.* 1981.)

been steam-generated at the vent by the interaction of magma and water.

Other types of pyroclastic fall deposit can resemble phreatoplinian deposits in the field. One is formed by local flushing of a downwind plinian or sub-plinian plume by atmospheric rain, and this type we have mentioned while discussing plinian deposits. Such an ash-fall deposit could contain accretionary lapilli, but an isopach map would show that the deposit only covered a very limited area. Co-ignimbrite ash-fall deposits associated with ignimbrite-forming eruptions (Chs 5 & 8) can be very widespread and, if rain-flushed, could also contain accretionary lapilli. However, these ash-fall deposits are vitric-enriched because crystals are preferentially segregated into the pyroclastic flows, while phreatoplinian deposits should contain nearer to the original magmatic crystal ratios if the magma were porphyritic. Texturally, co-ignimbrite ash-fall deposits should contain delicate shards and bubble wall fragments, suggesting fragmentation by exsolving magmatic gases. It has now also been recognised that plinian eruptions may produce substantially more fine ash than has hitherto been suspected, and may deposit poorly sorted, bimodal ashes distally. Problems in the interpretation of distal silicic ash layers are discussed in Section 6.9.

6.8.3 MECHANISMS

We have already discussed (Chs 3 & 5) some of the physical controls of phreatomagmatic or hydrovolcanic explosions that generate surtseyan and phreatoplinian pyroclastic fall deposits. Clearly, the major contrast between these types of eruptions and magmatic eruptions is the degree of fragmentation of the magma. In magmatic eruptions disruption and fragmentation of the magma is by exsolution and expansion of its volatiles. In comparison, this produces the relatively coarse population of particles observed in strombolian and plinian deposits. However, even in the phreatomagmatic case it is likely that some vesiculation and disruption of the magma occurs by magmatic gases. SEM studies do show that shards from surtseyan and phreatoplinian deposits, although having sharp fractured boundaries, may contain small vesicles, suggesting that magmatic fragmentation could play a role (see Figs

3.18, 24 & 25; Section 3.5.1). Self and Sparks (1978) suggested a two-stage model for fragmentation in many phreatomagmatic eruptions. Magma is first partially fragmented by vesiculating magmatic gases to give a coarse population which then interacts with water. Hydrovolcanic explosions occur and a second stage of fragmentation is initiated, which is aided by the large surface area of magma presented to the water because of the initial magmatic breakage. Final grainsize characteristics of the ejecta will depend on the efficiency of mixing. From Figure 3.9 a water : magma mass ratio of 0.3 leads to the most efficient fragmentation. If almost complete hydrovolcanic fragmentation occurs, the only evidence of the role of magmatic fragmentation will be small vesicles seen within some larger shards. In less-efficient events, larger ash-sized fragments may be poorly vesicular. However, it is unlikely that abundant delicate cuspate shards and bubble wall fragments would be preserved. This two-stage model for fragmentation also explains the grainsize distribution of phreatoplinian deposits: the fine-grained unimodal population is generated by hydrovolcanic fragmentation, while the coarse-tail is of larger particles broken by magmatic processes.

Eruption columns for this type of activity are driven by rapid successions of hydrovolcanic explosions. Observations of the 1963 Surtsey eruption suggest that these occur every few seconds to tens of seconds (Thorarinsson *et al.* 1964). Each explosion at Surtsey thrust out black jets of ash and bombs, which occasionally reached heights of about 1 km. Finer particles were then taken to greater heights by convection, occasionally as high as 9 km (Thorarinsson *et al.* 1964). During the 1979 Soufrière eruption, columns from phreatomagmatic explosions rose as high as 18 km (Sparks & L. Wilson 1982).

As the steam–pyroclast mixture rises, condensation of the steam may occur in the column. This phase change requires a large change in volume, and a substantial increase in density. Although this may be partially compensated for by mixing of air from the side of the column, partial collapse of the column could occur. It is in this situation that base surges (Ch. 5) will form. Eruptions producing large amounts of steam may have lower convective plumes, because of the thermal energy lost in vaporising water (Ch. 5). However, the much finer-grained nature of the ejecta means that it will be more widely dispersed from a lower plume than it would be from an entirely magmatic plume.

There are no direct observations of phreatoplinian eruptions, but the continuous eruption of rhyolitic magma at a high discharge rate through, say, a caldera lake is likely to produce an eruptive plume some tens of kilometres high.

6.9 Distal silicic air-fall ash layers

The interpretation of distal (> >150 km from the vent) air-fall ashes associated with large magnitude silicic eruptions has become problematical. Large magnitude events, in many cases ignimbrite-forming, can be very complex, and this makes understanding their distal ash layers difficult. Up to a few years ago they were generally assumed to be pre-ignimbrite air-fall deposits, a view still upheld by Izett (1981). More-recent studies have indicated that crystal-enriched ignimbrites should be accompanied by equally voluminous vitric-enriched ash falls. Many widespread ashes were subsequently interpreted as co-ignimbrite ash-fall deposits (e.g. Sparks & Huang 1980; Ch. 8). Widely dispersed phreatoplinian ash-fall deposits were then recognised, and G. P. L. Walker (1980) suggested that widespread ash layers could also be formed by littoral explosions when hot pumice flows entered the sea (see Chs 3, 9 & 10).

New studies, in which the total grainsize populations of deposits have been determined, now suggest that the volume of fine ash produced during plinian eruptions is much more than was previously supposed. Thus, the importance of widespread ash-fall deposits of plinian origin may have been underestimated.

6.9.1 WHOLE-DEPOSIT GRAINSIZE POPULATIONS

Most studies of pyroclastic fall deposits only provide data on thickness and grainsize to distances <150 km from the vent. Whole-deposit grainsize

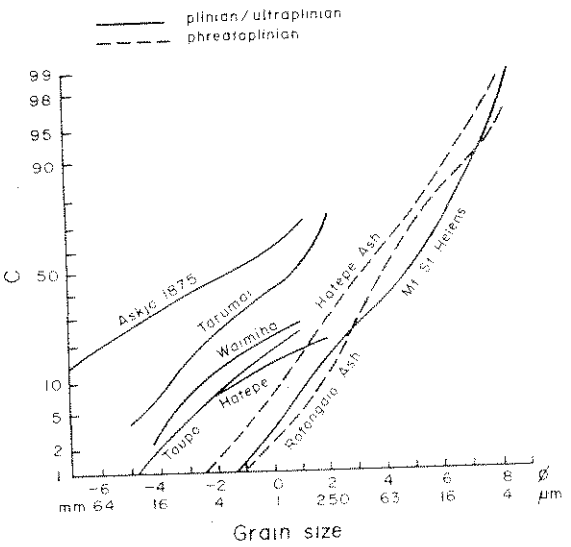

Figure 6.38 Whole-deposit grainsize populations of some pyroclastic fall deposits formed by highly explosive silicic eruptions. C is weight percentage coarser than size stated on the x-axis. (After G. P. L. Walker 1981e and Carey & Sigurdsson 1982.)

populations are important because they reflect the initial size distribution in the eruption column. The main problem has been to estimate the amount of fine-grained ash, because a proportion of this is always going to be deposited outside the limits of the minimum thickness isopach. Various methods have been employed, but usually they involve dividing the isopach map up into different segments. Grainsize data for the segments are averaged and then weighted according to the volume of each sub-unit. Crystal concentration studies are used to assess the total volume of the deposit for the area outside the minimum isopach (see App. I). The total grainsize distribution is then determined by integrating these data.

Whole-deposit grainsize curves for some deposits of highly explosive eruptions are given in Figure 6.38. What is surprising is the high proportion of fines found in some plinian deposits, and the Taupo ultraplinian deposit. These only seem to differ from the phreatomagmatic deposits in having a tail of coarser grainsizes, suggesting that fragmentation during plinian eruptions may be much greater than was previously thought. G. P. L. Walker (1981a) suggested that the markedly different appearances of plinian and phreatoplinian deposits in the field reflect a different depositional process, perhaps water-flushing in the second case, rather than degree of fragmentation.

The data from Mt St Helens (Fig. 6.38) are difficult to assess. Near the vent the air-fall is a somewhat typical coarse-grained plinian pumice deposit. However the whole-deposit grainsize population resembles that of phreatoplinian deposits, and a very high proportion of ash was produced during the eruption. Carey and Sigurdsson (1982) suggested that interaction with external water may have been important. However, mechanisms of magma fragmentation and how they operate during explosive eruptions are little understood at present. As indicated by G. P. L. Walker (1981a), the clarification of grainsize relationships requires more work.

6.9.2 SECONDARY THICKENING AND BIMODALITY

As well as large amounts of fine-grained ash, the Mt St Helens deposit surprisingly showed secondary thickening beyond the 1 cm isopach (Fig. 5.8c). First, the air-fall deposit thinned exponentially to 1.0 cm thickness at 180 km, but then increased to 4.0 cm thickness at 300 km before thinning once again at greater distances. Carey and Sigurdsson (1982) attributed this to premature fall-out of aggregated particles in the eruption plume. Sorem (1982) described ash clusters carefully collected while settling, and shows SEM photographs of these. These ashes are poorly sorted and bimodal. Aggregation may be related to condensation of vapour in the plume, which could have been important if water was involved in the eruption, or perhaps to electrostatic charging of particles.

Secondary thickening had previously only been described in the air-fall deposit erupted from Quizapu in 1932 (Larsson 1936), but Brazier *et al.* (1983) recognised that secondary thickening and bimodality may be common features of distal ash deposits. They describe several North American examples. Some are the distal deposits of ignimbrite-forming eruptions, but others were from solely plinian eruptions.

Bimodality has been used as a criterion to distinguish co-ignimbrite ashes from precursor plinian ashes in the deposits of multi-phase ignimbrite-forming eruptions. In co-ignimbrite ashes at or near vent, bimodality has been attributed to two separate sources which contribute the different modes (Sparks & Huang 1980; Ch. 8). The results from Mt St Helens and other North American ash layers now bring into question some of these interpretations. Bimodality may also be a common feature of distal plinian deposits. Volcanological considerations still support the idea that distal ash layers have a substantial co-ignimbrite component (cf. Izett 1981), but the plinian component may be much larger than was recently thought.

It is therefore apparent that, in distal situations, clearly distinguishing phreatoplinian, plinian and co-ignimbrite ash-fall deposits is going to be very difficult. By grainsize characteristics alone this may be impossible. Proximal characteristics of the deposits and the eruption sequence will provide the best criteria.

Finally, if secondary thickening is a common feature of distal plinian deposits, it therefore has important implications for calculating their volumes. Conventional ways of estimating the volumes of plinian deposits are based on thickness–distance plots. These plots give straight-line or exponential relationships in areas near the source (<150 km from the vent). However, secondary thickening in distal deposits suggests that this method is therefore unsuitable where dispersal of ash occurs over distances greater than 150 km from the vent (cf. Froggatt 1982). The volumes quoted in Table 6.2 were obtained by a different method (see App. I).

6.10 Welded air-fall tuffs

As discussed more fully in Chapter 8 (Section 8.10.1), welding involves the sintering together of hot, glassy fragments, irrespective of shape and size, under the influence of a compactional lithostatic load. During welding the glassy fragments deform plastically, producing a bedding parallel

Table 6.5 Examples of welded air-fall tuffs found on modern volcanoes.

Deposit	Composition	Reference
Thera welded tuff, Santorini	dacite (mixed)	Sparks & Wright (1979)
Therasia welded tuff, Santorini	dacite (mixed)	Sparks & Wright (1979)
Askja 1875, Iceland	rhyolite (mixed)	Sparks & Wright (1979)
Ruapehu, New Zealand	andesite	personal observation
Newberry caldera, Oregon, USA	andesite	personal observation
Mt Giardina, Lipari	rhyolite	personal observation
Krakatau 1883	dacite (mixed)	Self & Rampino (1981)
Mt St Helens 1980	dacite	Banks & Hoblitt (1981), Rowley *et al.* (1981)
Tenerife (several of the 'eutaxites')	phonolite	G. P. L. Walker (*pers. comm.*)
Green tuff, Pantelleria	pantellerite	J. V. Wright (1980), Wolff and Wright (1981, 1982)
Mayor island, New Zealand	pantellerite	B. Houghton (*pers. comm.*)
Mt Suswa 'globule tuff', Kenya	pantellerite	Hay *et al.* (1979)*
Tongariro, New Zealand	basaltic	Healy (1963)
Tarawera 1886, New Zealand	basaltic	Cole (1970), G. P. L. Walker *et al.* (1984)

* The description given by Hay *et al.* (1979) of this deposit suggests it is a welded air-fall tuff. In particular, the deposit is sheet-like, mantles topography, is frequently stratified, welded tuff is found interbedded with air-fall pumice close to the vent, and the overall degree of welding shows a strong dependence on distance from source.

fabric of flattened, elongate large pumice fragments (**fiamme**) and glass shards, known as **eutaxitic** texture.

Welded tuffs are common in the geological record, and are generally called ignimbrites or ash flow tuffs, implying deposition from a pyroclastic flow. However, welded air-fall tuffs are a common volcanic product, and are known to occur on several modern volcanoes, covering nearly the full range of magma compositions (Table 6.5). They have also been recognised in ancient volcanic successions (Suthren & Furnes 1980).

The best documented examples so far are from Santorini volcano, Askja volcano, Iceland (Sparks & Wright 1979) and the island of Pantelleria in the Channel of Sicily (J. V. Wright 1980). These tuffs can be distinguished from welded rocks formed from pyroclastic flows by their geometric form, textures and field relations to non-welded counterparts. Their features indicate post-emplacement compaction and welding over a wide area, and cannot simply be ascribed to the agglutination of spatter lumps on impact. We would restrict the use of the term 'agglutination' to describe the process of deformation and sintering of air-fall pyroclasts when they impact on an accumulating bed. Flattening is thus caused by the momentum of the falling pyroclasts. This is distinct from welding, in a strict sense, which occurs under the influence of load pressure imposed by already accumulated tephra on the underlying, still hot, part of the deposit. Agglutination requires the eruption of more fluid magma and, as we have discussed, is therefore a more important process in basaltic eruptions (Section 6.3). However, extensive welded scoria-fall deposits are known (Table 6.5), and agglutination could have been an important process near the vent during these eruptions.

Welding has also been documented in *'fused'* or *'sintered' tuffs*, where lava has induced welding of underlying air-fall layers (Christiansen & Lipman 1966, Schmincke 1967a), but these are not formed by primary processes like the examples described here.

6.10.1 CHARACTERISTICS AND EXAMPLES

Discussion of the more general aspects of welding textures and processes will be left until we describe welded ignimbrites in Chapter 8.

In the air-fall examples that are known, welding occurs outwards to a distance of 1–7 km from the probable vent position. Ignimbrites, on the other hand, can be welded at distances of 50 km or more from the source. The basic criteria used to distinguish welded tuffs of air-fall rather than pyroclastic flow origin are:

(a) mantle bedding and deposition on steep slopes (>20°; Fig. 6.39).
(b) internal stratification and distinguishable fall units (this may be reflected by rapid fluctuations in the compaction profile) and
(c) non-welded equivalents having depositional and grainsize characteristics of airborne ejecta.

We will now briefly mention some of the examples that have been described.

The *Thera welded tuff* on Santorini forms a distinctive black, glassy, dacitic layer as much as 7 m thick (Figs 6.40–42), which in hand specimen has a well developed eutaxitic texture. It is exposed for more than 1.5 km in the caldera wall and must have originally covered at least 1 km^2. Laterally and vertically the welded tuff passes into a thick, coarse, non-welded pumice fall deposit (the Middle Pumice, Fig. 13.30) which, near the welded tuff, is thermally darkened and black in colour (Fig. 6.41). This layer mantles topography, and isopach and maximum-sized isopleth maps are typical for plinian air-fall deposits (cf. Figs 6.18 – 19). These maps indicate that the vent was near to the place where the welded tuff is thickest. On close inspection the tuff is seen to be internally stratified and to contain some conspicuous layers of coarse pink pumice. Many of these are not laterally continuous, and they are thought to have formed by the rapid local accumulation of very large pumice bombs. These produce anomalous deviations in the compaction profile, and one is shown in Figure 6.42. Grainsize analyses of the non-welded pumice deposit are typical of a fall deposit (Fig. 6.43).

The *Askja 1875 welded tuffs* were formed during

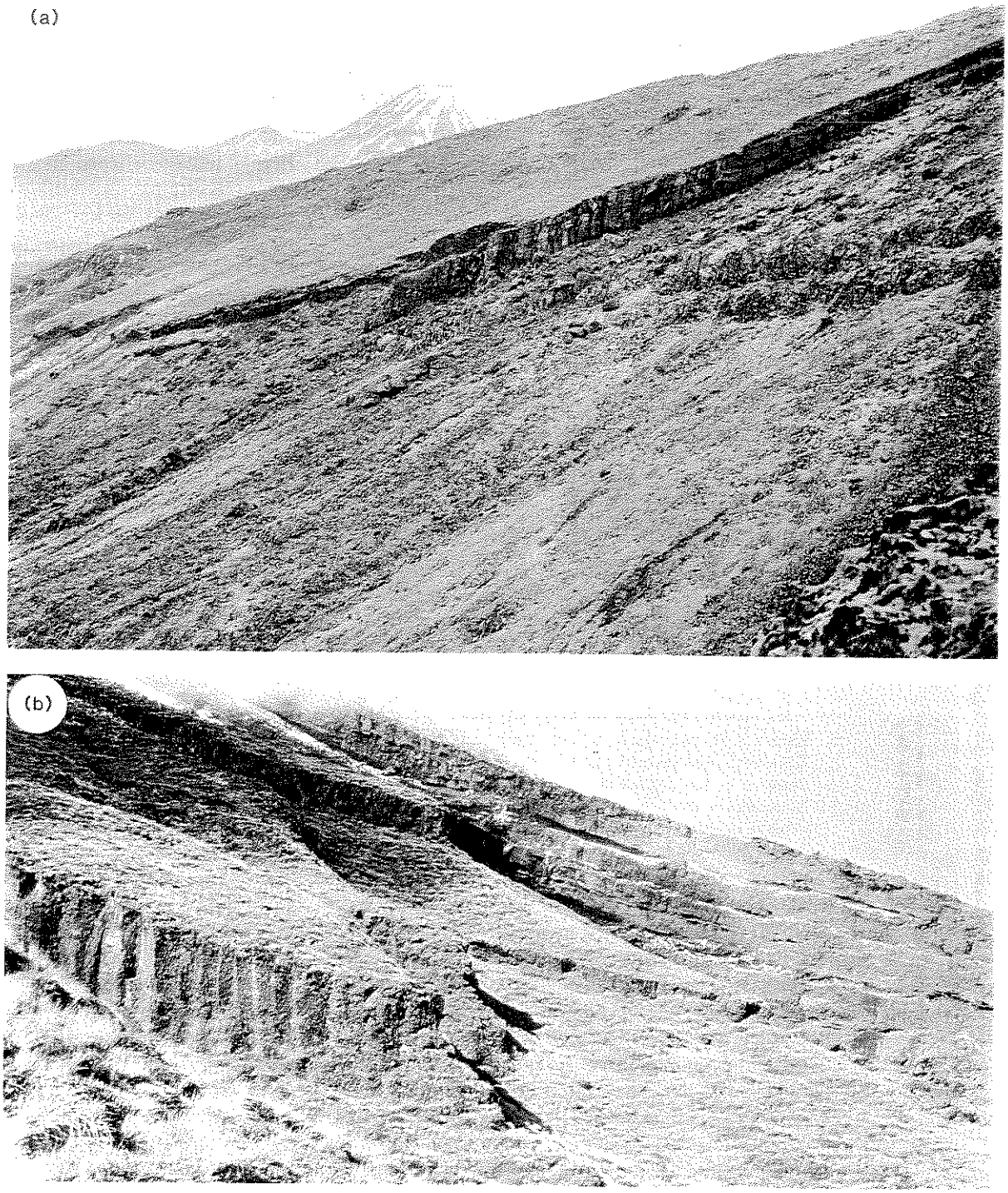

Figure 6.39 Welded air-fall tuffs mantling topography on (a) Ruapehu and (b) Tongariro volcanoes, New Zealand (both photographs by C. J. N. Wilson). Note vertical cooling joints in (b).

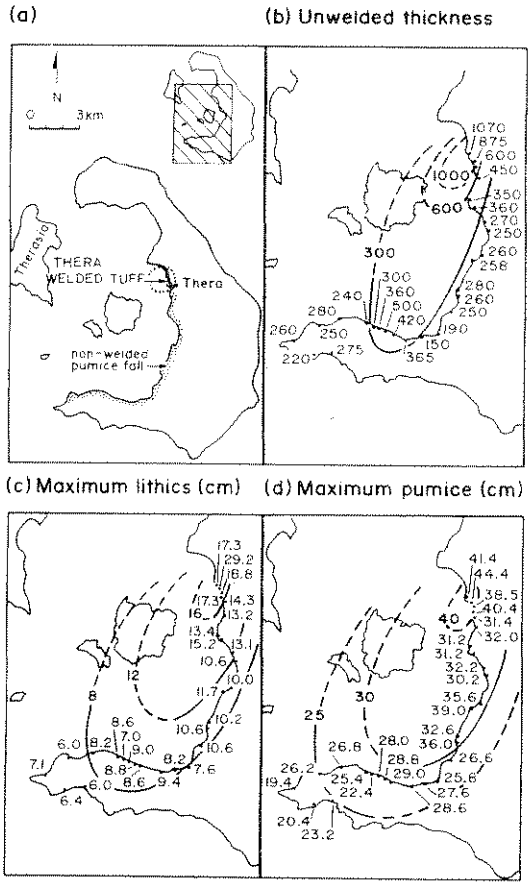

Figure 6.40 Distribution of the Thera welded tuff and its equivalent non-welded pumice-fall deposit (the Middle Pumice) in the caldera wall of Santorini, Greece. Dotted circle marks the area in which the source vent probably occurs. Isopleths show the average diameter of the five largest clasts. (After Sparks & Wright 1979.)

the same explosive rhyolitic eruption of this Icelandic volcano discussed previously in Section 6.4. The eruption produced a number of distinctive pyroclastic layers, and two of these (C and D in Fig. 6.33b) pass into welded rocks near Oskjuvatn caldera (Fig. 6.44). The most important welded tuff grades laterally into layer C_2 (Figs 6.44 & 45). This welded tuff has a maximum thickness of 4 m and covers a minimum area of 1.6 km^2. The welded tuff mantles topography and can be found on slopes as steep as 30°. It is stratified, and there are marked fluctuations in the compaction profile. Welded air-fall tuffs are deposited in layers, and can show vertical variations in grainsize, sorting, components and, more importantly, accumulation rate. This can result in more-irregular compaction profiles than with ignimbrites.

The *Green Tuff* of Pantelleria is the best-exposed and most spectacular and has been shown to have been of plinian proportions (Wolff & Wright 1982), and in its original distribution it must have mantled the entire island (85 km^2) with over 5 m of densely welded tuff. The tuff drapes the former topography (Figs 6.46 & 47), but is ponded in depressions due to **rheomorphism**, which is the post-depositional secondary flowage of welded tuff (Ch. 8). The overall geometry resembles that of pyroclastic surges or low aspect ratio ignimbrites (Ch. 8). However, there is no correlation between the degree of welding and the thickness, as might be expected were the thickness variation a primary flow feature.

Other welded tuffs on Pantelleria adhere to slopes steeper than 30°. A good example of a welded air-fall tuff in Figure 6.47d shows alternating layers of densely welded tuff and well sorted pumice, which are thought to reflect changes in accumulation rate during the eruption (J. V. Wright 1980).

6.10.2 CONDITIONS OF FORMATION

The critical problem posed by welded air-fall tuffs is to determine under what conditions airborne ejecta can remain sufficiently hot during flight to weld and compact after deposition. The basic controls are high discharge and accumulation rates. Field evidence suggests that accumulation rate is the critical factor. Both the Thera and Askja welded tuffs are thickest and most densely welded near the vent, where the accumulation rate was greatest (cf. welded ignimbrites which are again most densely welded where they are thickest, but where they are ponded in a depression this could be a long distance from the vent).

Accumulation rate has two main effects. First, rapid accumulation prevents radiative and convective cooling of deposited fragments. On burial, fragments are insulated, so they cool by conduction alone, which is a slow process because of the high

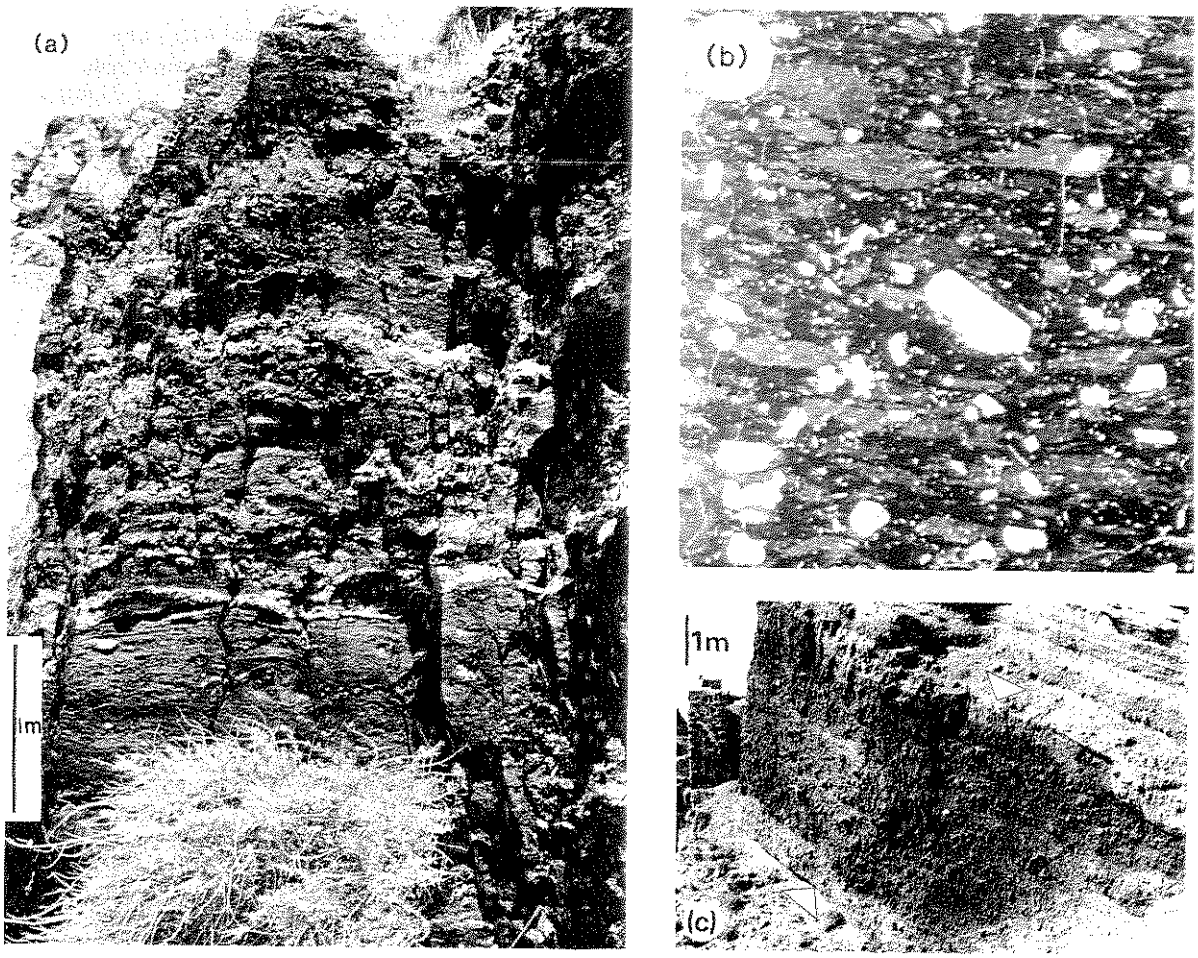

Figure 6.41 The Thera welded tuff, Santorini, Greece. (a) At Thera Harbour with well developed internal stratification. (b) Photomicrograph (negative) of eutaxitic texture. Note the development of perlitic cracking. Area shown is about 1 cm across. (c) Non-welded pumice fall (between arrows) which is the lateral equivalent. Note thermal darking above base.

Figure 6.42 Compaction and lithological profile through the Thera welded tuff, Santorini, Greece, where it is thickest. The minimum strain ratio assumes all ellipsoidal pumice clasts landed with their long axes parallel to bedding. (After Sparks & Wright 1979; see this paper for method of measuring strain ratio.)

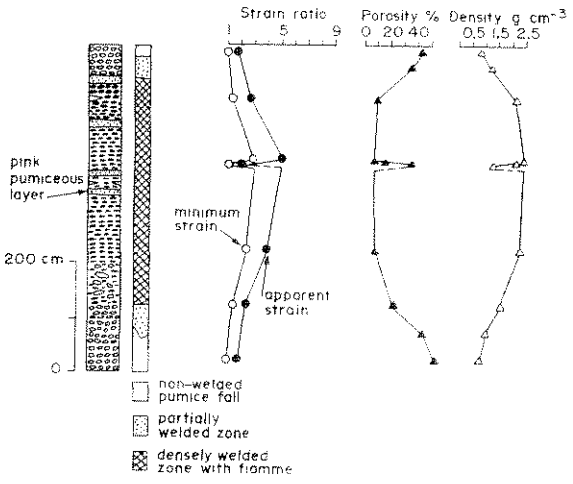

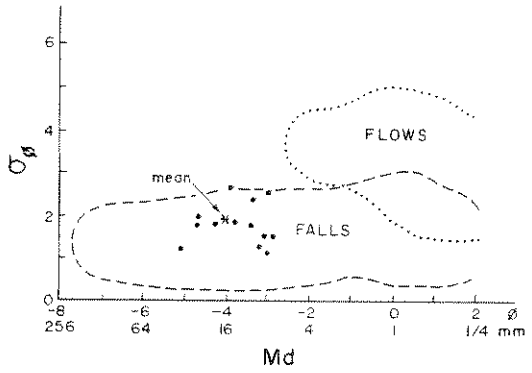

Figure 6.43 Md_ϕ/σ_ϕ plot of the non-welded part of the Thera welded tuff (for examples of grainsize histograms see Fig. 6.3). On the basis of grainsize (Ch. 12), this welded deposit and the other examples described herein would be classified as 'welded agglomerates' and 'welded lapilli tuffs'. For brevity in nomenclature, we have used 'welded tuff' as a general term to cover them all. (After Sparks & Wright 1979.)

porosity and poor conductivity of pumice. Secondly, rapid accumulation leads to lower heat losses by radiation, as a consequence of increasing concentrations of fragments per unit volume of air in the falling ejecta. At high temperature, an incandescent clast loses much of its heat by radiation. This loss is reduced if each particle is surrounded by other hot particles radiating heat in a dense cloud, as each particle absorbs radiated heat from its neighbours. The Askja 1875 eruption is sufficiently well documented to allow an estimate of the accumulation rates which produced the welded tuff (Sparks & Wright 1979). For the densely welded zone this was calculated as 20 cm min^{-1}, and at the boundary between incipiently welded and non-welded zones it was between 2 and 4 cm min^{-1}.

Both the Thera and Askja welded air-fall tuffs are also mixed pumice deposits (Sparks & Wright

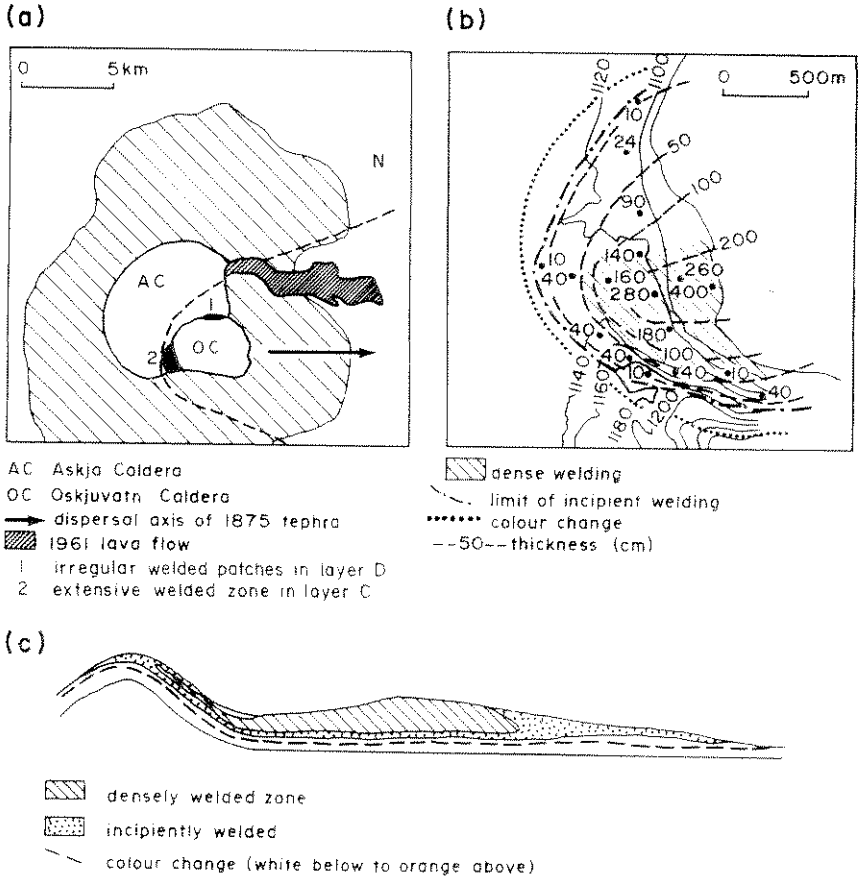

Figure 6.44 (a) Location of the welded tuff horizons from the 1875 Askja eruption, Iceland. (b) Isopach map of the layer C (Fig. 6.33) welded tuff. (c) Schematic north-south profile through layer C, showing relationships between welding zones and thermal colour changes. (After Sparks & Wright 1979.)

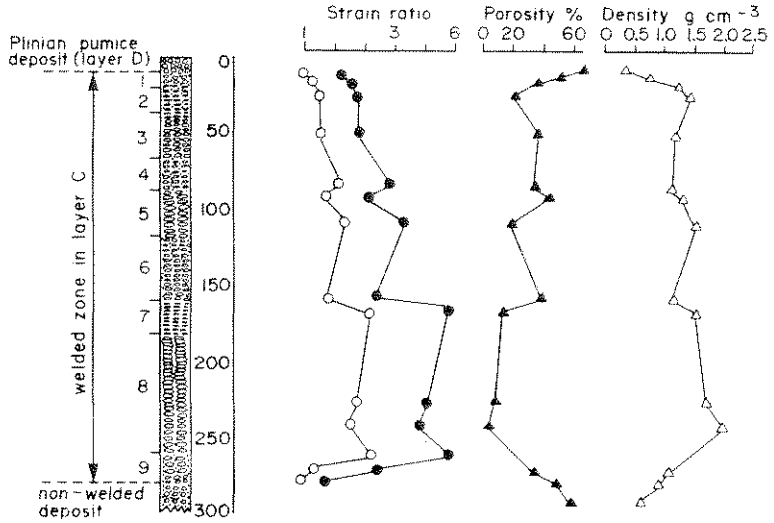

Figure 6.45 Compaction and lithological profile through the zone of densest welding at the thickest part of the Askja welded tuff. (After Sparks & Wright 1979.)

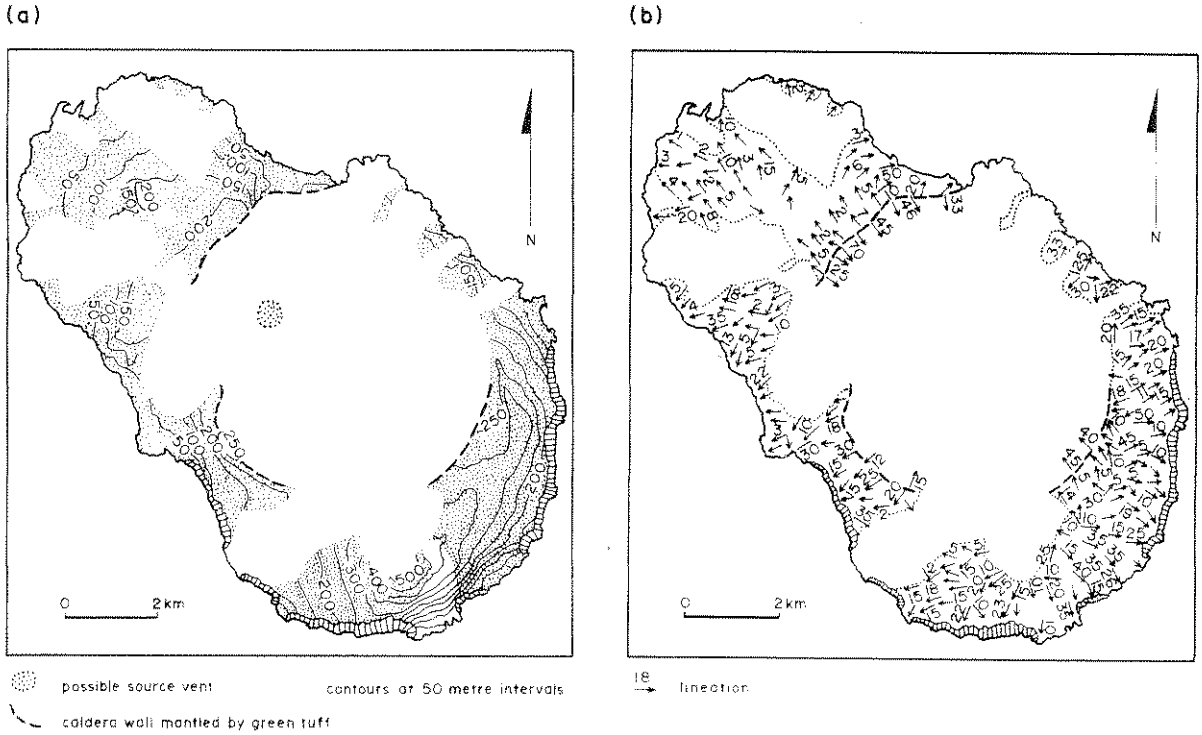

Figure 6.46 The Green Tuff, Pantelleria. (a) Present outcrop (stipple) and contours showing how the welded tuff mantles topography. (b) Generalised map of lineations produced by stretching of fiamme during secondary mass flowage (see Fig. 6.47b). (After J. V. Wright 1980 and Wolff & Wright 1981.)

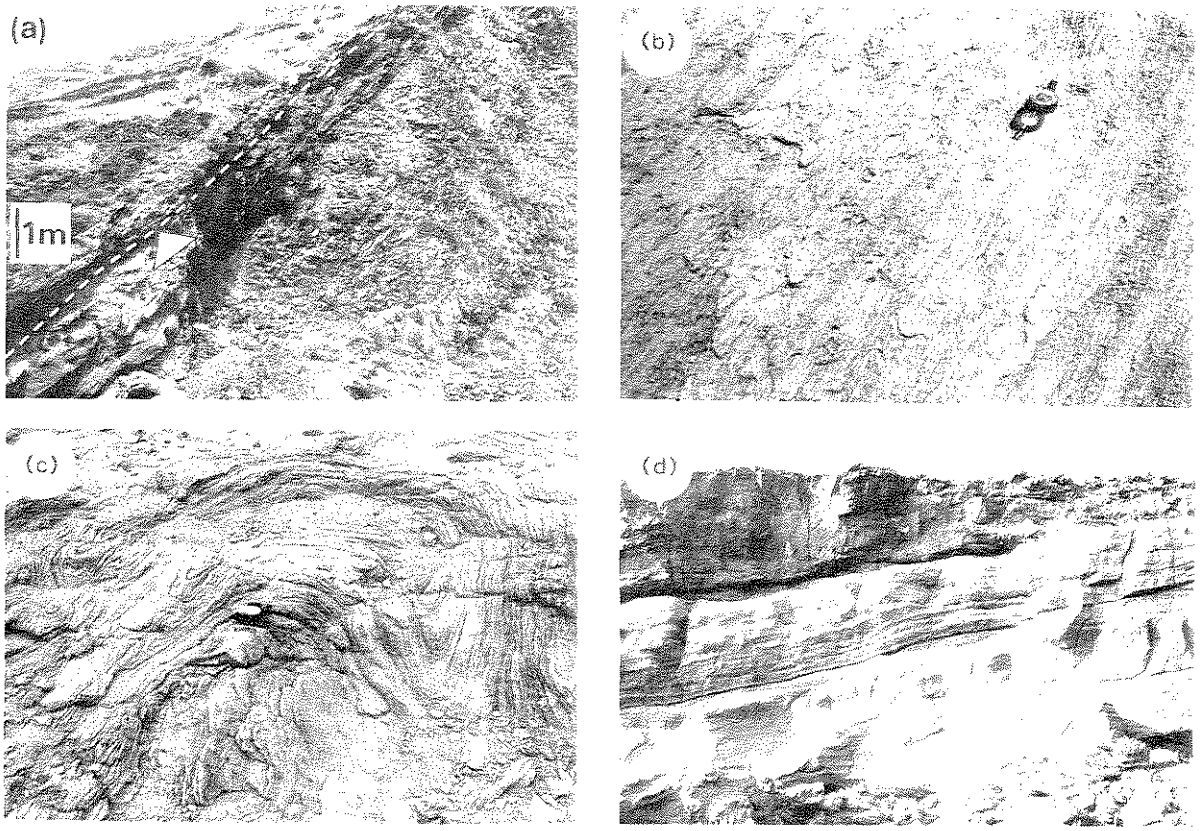

Figure 6.47 Welded tuffs on Pantelleria. (a) Two deposits mantling an older rhyolite lava dome. The uppermost (above arrow) is the Green Tuff, which has a slope of 40°. (b) Strong lineation in the Green Tuff produced during rheomorphism. (c) Refolded fold in the Green Tuff. (d) Welded air-fall tuff showing alternating layers of densely welded tuff (dark) and non-welded white pumice fall. This is overlain by a younger welded tuff (dark), which underlies the Green Tuff in (a). Section is 10 m thick.

1979). Superheating of the silicic component may have been an additional factor promoting welding. However, the importance of this is difficult to judge, because many pumice fall deposits show evidence of magma-mixing but are not welded.

Wolff and Wright (1981, 1982) suggested that compositional factors have favoured the formation of widespread and rheomorphic welded air-fall tuffs on Pantelleria. Due to the low viscosity of pantelleritic ejecta, dense welding can occur at moderate accumulation rates, and Wolff and Wright (1982) indicated a rate of the order of 1 cm min^{-1} for the Green tuff.

6.10.3 THERMAL FACIES MODEL

It is now possible to suggest a thermal facies model for pyroclastic fall deposits. This scheme is shown in Table 6.6. The lateral changes indicated also occur vertically; most of the welded examples that we have described display a range of these facies in the vertical section. What is evident from this type of analysis is the overlap between pyroclastic processes and some lava-forming processes. However, considerable uncertainty must be attached to the interpretation of clastogenic lava facies. Although this is a common facies found in the products of basaltic eruptions, it is unlikely to be found in those of more-silicic magmas. A rhyolitic agglutinate is known to us at Panum

Crater, Mono Craters, but more generally these features in high-silica rocks are only going to be found in the fluidal ejecta derived from peralkaline magmas. Pantelleritic clastogenic lavas may occur on Mayor Island, New Zealand (B. Houghton *pers. comm.*).

The rheomorphic facies again seems rare among silicic air-fall deposits. At present it has only been described from Pantelleria (J. V. Wright 1980, Wolff & Wright 1981, 1982), but other pantelleritic welded air-fall tuffs on Mayor Island and Suswa (Table 6.5) show secondary flowage. Rheomorphism has also been noted in an andesitic welded air-fall tuff on Ruapehu volcano, New Zealand (Fig. 6.39a & Table 6.5), and in some Icelandic rhyolitic welded air-fall tuffs (H. Sigurdsson & O. Smarason *pers. comms*). These include the Askja welded air-fall tuff, which shows some incipient rheomorphic structures.

Basaltic pyroclastic fall-forming eruptions often seem to produce deposits showing a complete range of thermal facies. In contrast, pumice fall deposits are generally non-welded, with no welded facies present. However, if non-welded they may still show some thermal effects. Grey, black or brown zones of thermal darkening may occur, and care should therefore be taken when interpreting dark-coloured pumice because this may not necessarily indicate a more basic composition.

Table 6.6 Suggested thermal facies model for pyroclastic fall deposits.

	(1) Clastogenic lava	(2) Rheomorphic welded tuff	(3) Densely welded tuff	(4) Partially welded tuff	(5) Non-welded pumice deposit
	increasing distance from vent →				
	decreasing accumulation rate →				
	decreasing temperature →				
major process(es)	agglutination rheomorphism	load-pressure welding, rheomorphism	load-pressure welding	load-pressure welding	
minor process(es)	load-pressure welding	agglutination			
characteristic texture or structure	massive lava rock; relict clast structures	linear fabric; flow-folds	planar fabric or eutaxitic texture; *near-zero porosity* in zone of densest welding	poorly developed eutaxitic texture, relict primary porosity	loose pumice
examples		Mt Suswa 'globule tuff'			
		Green Tuff, Pantelleria			
			Askja 1875		
			Thera welded tuff		
				Krakatau 1883	
	Tarawera 1886				

6.11 Further reading

G. P. L. Walker (1973b) is essential reading, and forms the basis for much of our treatment of pyroclastic fall deposits. Also highly recommended is the review by G. P. L. Walker (1981b) of plinian fall deposits. The series of papers entitled 'Explosive volcanic eruptions I–V' (G. P. L. Walker *et al.* 1971, L. Wilson 1972, 1976, L. Wilson *et al.* 1980, Sparks & L. Wilson 1982) provides a sound physical basis for understanding pyroclastic fall-producing eruptions. L. Wilson and Head (1981) is again recommended for a quantitative analysis of basaltic explosive mechanisms. Further physical treatment of pyroclastic falls is found in Allen (1982), while Fisher and Schmincke (1984) also discuss processes and the characteristics of the deposits.